THE JOURNAL OF COMPARATIVE NEUROLOGY 291:281-304 (1990)

GABA-ergic and Glycinergic Pathways in the Inner Plexiform Layer of the Goldfish Retina

JAY F. MULLER AND ROBERT E. MARC
Department of Physiology, University of Utah School of Medicine, Salt Lake City, Utah 84108 (J.E.M.); Sensory Sciences Center, University of Texas Graduate School of Biomedical Sciences, Houston, Texas 77030 (R.E.M.)

ABSTRACT

GABA-ergic and glycinergic circuitry in the inner plexiform layer of the goldfish retina was evaluated by electron microscopic autoradiography of ^{3}H-GABA and ^{3}H-glycine uptake, combined with retrograde horseradish peroxidase (HRP) labeling of ganglion cells. GABA-ergic and glycinergic synapses were found on labeled ganglion cells throughout the inner plexiform layer. This reinforces the idea that physiological evidence of GABA-ergic and glycinergic influence on a variety of ganglion cells in goldfish and carp often reflects direct inputs. Double-labeled synapses are presented as evidence of direct type Ab amacrine cell input to on-center ganglion cells. At least one population of type Aa sustained-off GABA-ergic amacrine cell is proposed, on the basis of profuse GABA-ergic inputs onto bipolar cells in sublamina a. Similar GABA-labeled profiles are shown to synapse onto HRP-labeled probable off-center ganglion cells. Thus GABA-ergic amacrine cells not only provide the predominant feedback to depolarizing (on-center) and hyperpolarizing (off-center) bipolar cells but also provide feed-forward inputs to on- and off-center ganglion cells. Large-caliber GABA-ergic dendrites present in both sublaminae a and b resemble those expected of a previously described bistratified, transient amacrine cell. These processes synapse onto HRP-labeled ganglion cell profiles in both sublaminae. Two morphologies of glycinergic amacrine cell are proposed on the basis of light microscopic autoradiography, 1) the previously described small pyriform cell and 2) a multipolar cell. The differential connectivity of the glycinergic neurons described, however, remains indistinguishable. Whereas abundant glycinergic inputs to ganglion cells occur throughout the inner plexiform layer, contacts between glycinergic profiles and bipolar cells are extremely rare. Therefore, interpreting the meaning of glycinergic input to ganglion cells will require further study of amacrine cell circuitry.

Key words: amacrine cells, ganglion cells, autoradiography, horseradish peroxidase, neuronal circuitry

The specific connectivity of retinal neurons underlies image coding by the visual system. All vertebrate retinas share a neuronal architecture composed of photoreceptors, horizontal cells, bipolar cells, amacrine cells, and ganglion cells; the projections of these cells within the retina form the outer and inner plexiform layers. It is the variety of cell types within each class that gives rise to the diversity of retinal information coding. The present work concerns the components that interact in the inner plexiform layer of the goldfish retina.

In vertebrates, as is well known, the inner plexiform layer can be divided into a distal region, closer to the amacrine cell layer (sublamina a), and a proximal region, near the ganglion cell layer (sublamina b). In general, components of off-center pathways synapse in sublamina a and those of the on-center pathway in sublamina b (Famiglietti and Kolb,

Accepted August 23, 1989.

'76; Famiglietti et al., '77; Nelson et al., '78). Although there are differences among vertebrates regarding to what extent the various subtypes of bipolar cells and amacrine cells fit the sublamina a/sublamina b model, ganglion cells appear to fit in all species studied (Kolb, '82; Kolb and Nelson, '84). In fishes, the terminals of hyperpolarizing mixed rod-cone bipolar cells are in sublamina a, and depolarizing mixed rod-cone bipolar cells clearly terminate in sublamina b. Accordingly, they are abbreviated as Ma and Mb bipolar cells (Famiglietti et al., '77; Ishida et al., '80; Kaneko et al., '79, '80, '81; Saito et al., '83, '84, '85). Furthermore, in fishes, sustained-hyperpolarizing amacrine cells generally stratify in sublamina a and sustained-depolarizing amacrine cells generally stratify in sublamina b; we refer to them as Aa and Ab amacrine cells, respectively (Famglietti et al., '77; Kaneko et al., '79; Teranishi et al., '84, '85, '87; Djamgoz et al., '85; Djamgoz, '86; Djamgoz and Wagner, '87). Transient, on/off amacrine cells and ganglion cells, which respond briefly at stimulus onset and offset, stratify either along the sublamina a/b border or, more often, in both sublaminae a and b (Famiglietti et al., '77; Teranishi et al., '84, '85, '87; Djamgoz et al., '85; Djamgoz, '86; Djamgoz and Wagner, '87).

In teleostean fishes (Famiglietti et al., '77; Naka, '77) and mudpuppy (Frumkies et al., '81; Miller and Dacheux, '76), the basic design of parallel pathways through the retina has been well established. Intracellular current injection combined with extracellular recording showed that depolarizing bipolar cells in catfish drive on-center ganglion cells through a sign-conserving path; off-center ganglion cells were likewise driven by hyperpolarizing bipolar cells (Naka, '77). In mudpuppy, the on- and off-center pathways were found to be separable by low-chloride blockade of the on-center pathway (Miller and Dacheux, '76), and pharmacological blockade, by glutamate analogues, of either on or off pathways (Slaughter and Miller, '81, '83).

In fishes, ganglion cells are GABA and glycine-receptive (Cohen and Fain, '88; Ishida and Cohen, '88) and, as in other vertebrates, GABA and glycine have been found to influence on-center, off-center, and on/off ganglion cells (Negishi et al., '78; Djamgoz et al., '81; Glickman et al., '82). This is reflected anatomically; the sum of putatively GABA-ergic and glycinergic neurons makes up the majority of amacrine cells (Marc et al., '88; Miller, '88; Marc, '89). In cyprinid fishes, the two primary strategies for marking GABA-ergic and glycinergic neurons have been 1) high affinity uptake of radiolabeled GABA, GABA analogs, and glycine, followed by autoradiographic analysis (Lam and Steinman, '71; Marc et al., '78, '88; Marc and Lam, '81; Marc, '82, '89; Marc and Liu, '84; Ayoub and Lam, '84; Ball and Brandon, '86; Yazulla et al., '84; Yazulla, '86; Ball, '87; Muller and Marc, '88), and 2) immunocytochemical localization of GABA-ergic probes: GABA-like and glutamic acid decarboxylase (GAD)-like immunoreactivity and glycine-like immunoreactivity (Lam et al., '79, '85; Brandon, '85; Ball, '87; Studholme and Yazulla, '87, '88; Marc et al., '88). Correlations of autoradiographic and immunocytochemical data have been important recent strategies for ascertaining the neurochemical identities of retinal neurons. With certain notable exceptions to be discussed later, there has been good correspondence between probes. It has also become apparent that both GABA-ergic and glycinergic amacrine cells are heterogeneous populations, composed of distinct subtypes.

We have employed retrograde transport of horseradish peroxidase (HRP) as a structural label for ganglion cells and high-affinity uptake of radiolabeled GABA and glycine as neurochemical markers for amacrine cells. Combining easily distinguishable ultrastructural markers for amacrine cells and ganglion cells is advantageous. Otherwise, delineating amacrine cell from ganglion cell profiles without extensive reconstruction can be risky, particularly with recent evidence from catfish that some ganglion cells may be presynaptic in the inner plexiform layer (Sakai et al., '86). In the present study, HRP-labeled ganglion cells were selected for their dendritic stratification patterns; they correlate to on-center, off-center, and on/off physiological types (Famiglietti et al., '77). By adding autoradiographic markers for GABA and glycine, we have sought further insight into how GABA-ergic and glycinergic interneurons can directly influence on-center, off-center, and on/off signal pathways.

MATERIALS AND METHODS

The double-label employed herein has allowed two general alternatives for analysis: 1) serial sectioning and electron microscopic (EM) autoradiography of well isolated HRP-labeled ganglion cells whose dendritic arbors are solidly filled and 2) sectioning retinal regions with dense fields of solidly labeled ganglion cells and processing them for EM autoradiography. Double-labeled synapses can then be surveyed throughout the inner plexiform layer for both an overall distribution of inputs onto ganglion cells and selected patterns of input to individual cell types. We express the location of a feature in the inner plexiform layer as a percent distance from the amacrine cell layer border: level 0 (L0) to the ganglion cell layer border: Level 100 (L100). Sublayers 1–5 are equal subdivisions (each 20% intervals); sublayer 1 begins at L0, and sublayer 5 ends at L100 (Marc, '86).

Anesthesia and HRP injection

Goldfish (*Carassius auratus*), 8–15 cm in standard length, were secured dorsal side up with sponge in an ice bath, and anesthetized by respiration with 0.01–0.02% MS222 (tricaine methanesulfonate) or 4% benzocaine in acetone diluted 1:500 with water. Optic nerves were exposed by cutting a notch in the dorsal cartilage, rostromedial to the orbit (avoiding the major blood vessels leading from the gills). The optic nerves were injected with a 10 μl Hamilton syringe containing 25–30% Sigma VI or Boehringer-Mannheim grade I HRP in 2% aqueous dimethyl sulfoxide, within 2–3 mm of the eye. The injection site was plugged with HRP-soaked Gelfoam, and the surgical area was filled with Aquaphor gel for protection. Fishes were revived by respiration with oxygenated water, keeping the gills free and moist until normal head and tail movements were seen, for a survival time of 20–48 hours.

Isolated retina preparation: Incubation in ^{3}H-neurotransmitter and fixation

As the last part of the survival time, fishes were dark-adapted, usually overnight, to facilitate retinal isolation. Fishes were cervically transected and pithed, and the eyes were removed and hemisected. The eyecup was quartered, and the retinal portions were freed in cold, oxygenated teleost saline: 150 mM NaCl, 5 mM Hepes, 3 mM KCl, 2.1 mM $CaCl_2$, 1.4 mM $MgSO_4$, 1.4 mM $NaHCO_3$, 0.7 mM NaH_2PO_4, 10 mM glucose. In certain preparations the saline was nutrient-fortified according to Ames and Nesbett ('81). Each quarter retina was incubated for 10 minutes in a 25 or 50 μl droplet of 2–6 μM concentrations of ^{3}H-GABA, (specific activity [S.A.] 25–50 Ci/mMole) or ^{3}H-glycine (S.A.

16–20 Ci/mMole) in teleost saline, in a moist, oxygenated environment. Isotopes were obtained from New England Nuclear (Boston, MA). In several preparations 1 mM nipecotic acid (Sigma), a competitive inhibitor of GABA uptake, was added to the ^{3}H-GABA incubation medium. Nipecotic acid counteracts the spatial buffering effect caused by the high density of GABA uptake sites in the inner and outer plexiform layers (Marc, '86, '89; Marc et al., '88). Similar concentrations of unlabeled GABA added to the incubation medium would be equally effective in improving ^{3}H-GABA's access to the entire inner plexiform layer (Marc et al., '88; Marc, '89). Nipecotic acid was chosen for the present study because it is not metabolized after uptake (Madtes and Redburn, '85), nor does it specifically bind to GABA receptors (Redburn et al., '83). After a 30 second saline rinse, retinas were fixed in a freshly prepared fixative: 1% paraformaldehyde, 2.5% glutaraldehyde, 0.012% $CaCl_2$, and 3% sucrose in 80 mM sodium cacodylate buffer, at pH 7.4, after which they were rinsed several times in 0.16 M sodium cacodylate (pH 7.4) and left overnight in 0.16 M sodium cacodylate with 5% sucrose. Unless otherwise specified, all preparations were done at room temperature, and the buffer used was 0.16 M sodium cacodylate.

HRP development and histology

After a brief buffer rinse, the fixed samples were developed for HRP content with diaminobenzidine tetrachloride (DAB). All samples were presoaked, with rotation, for 30–45 minutes in a filtered solution of 0.08–0.1% DAB, 0.02–0.03% cobalt chloride, and nickel ammonium sulfate in buffer (Adams, '81). Hydrogen peroxide was added to a final concentration of 0.02%, and the samples were incubated for an additional 30–45 minutes. Some samples, after a short buffer rinse, were then incubated for 30 minutes in a 0.15% Hanker-Yates reagent (Polysciences) in buffer with 0.02% hydrogen peroxide (Muller and Marc, '84).

The samples were buffer rinsed and postfixed in buffered 1% osmium tetroxide. In some experiments 0.1–0.15% potassium ferricyanide was added to the osmium tetroxide for postfixation at 4°C in the dark. Later we found that 1% osmium tetroxide for 40 minutes followed by 1% osmium tetroxide with potassium ferricyanide for 30 minutes may be preferable (Wong-Reilly and Kageyama, '85). After a rinse in buffer or deionized water, the retinal portions were dehydrated in a cold graded methanol series and acetone, embedded in a soft Polybed 812 (Polysciences) mixture (2:1 DDSA:Polybed 812, 2% DMP-30 by volume), and polymerized at 60–65°C 6 hours to overnight.

Serial 40 or 60 μm sections were cut on an American Optical sliding microtome, dipped in unpolymerized Polybed mixture, serially slide mounted, and polymerized as above. This section thickness range has been useful for camera lucida drawing, light microscopy with Nomarski optics, and remounting for thin sectioning. Most thick sections were vertical, but some samples were chosen for horizontal or near-horizontal sections. Sections were examined for ganglion cells whose cell bodies and dendrites were solidly filled with reaction product and well isolated from the labeled dendrites of other ganglion cells. From these isolated ganglion cells, examples were chosen primarily on the basis of their dendritic stratification. Camera lucida drawings were made of those individual HRP-labeled ganglion cells chosen for subsequent autoradiographic analysis. Several ganglion cells, viewed in slightly oblique sections, were drawn abstracted to the vertical by using landmarks such as the amacrine cell layer border and the ganglion cell–optic fiber layer border to sketch the dendrites at different planes of focus. The areas of the thick sections selected were remounted onto plastic blanks, either with rapid setting epoxy cement or unpolymerized Polybed, and resectioned on a Sorvall MT2B microtome for EM autoradiography.

Autoradiography

Retinal areas selected for EM autoradiographic analysis were screened by sectioning the same region of a neighboring section for light microscopic autoradiography. Semithin (0.5–1.0 μm) sections were deplasticized with sodium methoxide and coated with a 50% solution of Kodak NTB-2 photographic emulsion. After 1–4 weeks of exposure at 4°C, the slides were developed with Dektol or D-19 (Kodak) for 2 minutes and examined for silver grain density and localization. The sections were counterstained with dilute toluidine blue in sodium borate. On the basis of these results, final selections of labeled ganglion cells were made, and exposure times for EM autoradiography were set.

Silver-gold thin sections (70–80 nm) were cut with glass knives on a Sorvall MT2-B ultramicrotome and collected on slot grids coated with Parlodion film, stained with uranyl acetate and Reynolds' or Luft's lead citrate, and carbon-coated. A fresh stock of Parlodion solution, 0.5% in n-pentyl acetate, and a moderately heavy carbon coat are recommended to protect against film hydration and weakening during long exposures and from the rigors of development. The grids were then coated with a 1:2 dilution of Ilford L-4 photographic emulsion by using wire loops (Bouteille, '76). The emulsion-coated grids were mounted on slides with double-stick tape or Grid Sticks (Ted Pella, Inc.) and stored at 4°C in slide boxes containing desiccant packets for the desired exposure times.

In some experiments, a number of grids were first developed at 2–3 weeks with D-19 or Microdol-X (Kodak) for early assessment. However, physical development with phenidon (1 minute at 10–15°C), though requiring longer exposure times (5–10 weeks), produced more discrete silver grains, preferable for analysis of small labeled profiles. All electron microscope autoradiographic data presented in this study were drawn from phenidon-developed grids (Bouteille, '76).

Abbreviations

R	photoreceptor
ONL	outer nuclear layer
INL	inner nuclear layer
HC	horizontal cell
BC	bipolar cell
Ma	hyperpolarizing mixed rod-cone bipolar cell (type a, off-center)
Mb	depolarizing mixed rod-cone bipolar cell (type b, on-center)
ACL	amacrine cell layer
AC	amacrine cell
Aa	sustained hyperpolarizing amacrine cell (type a, off-center)
Ab	sustained depolarizing amacrine cell (type b, on-center)
on/off AC	transient, on/off amacrine cell
IPL	inner plexiform layer
a	sublamina a
b	sublamina b
GCL	ganglion cell layer
GC	ganglion cell
off GC	sustained off-center ganglion cell
on GC	sustained on-center ganglion cell
on/off GC	transient, on/off ganglion cell
OFL	optic fiber layer

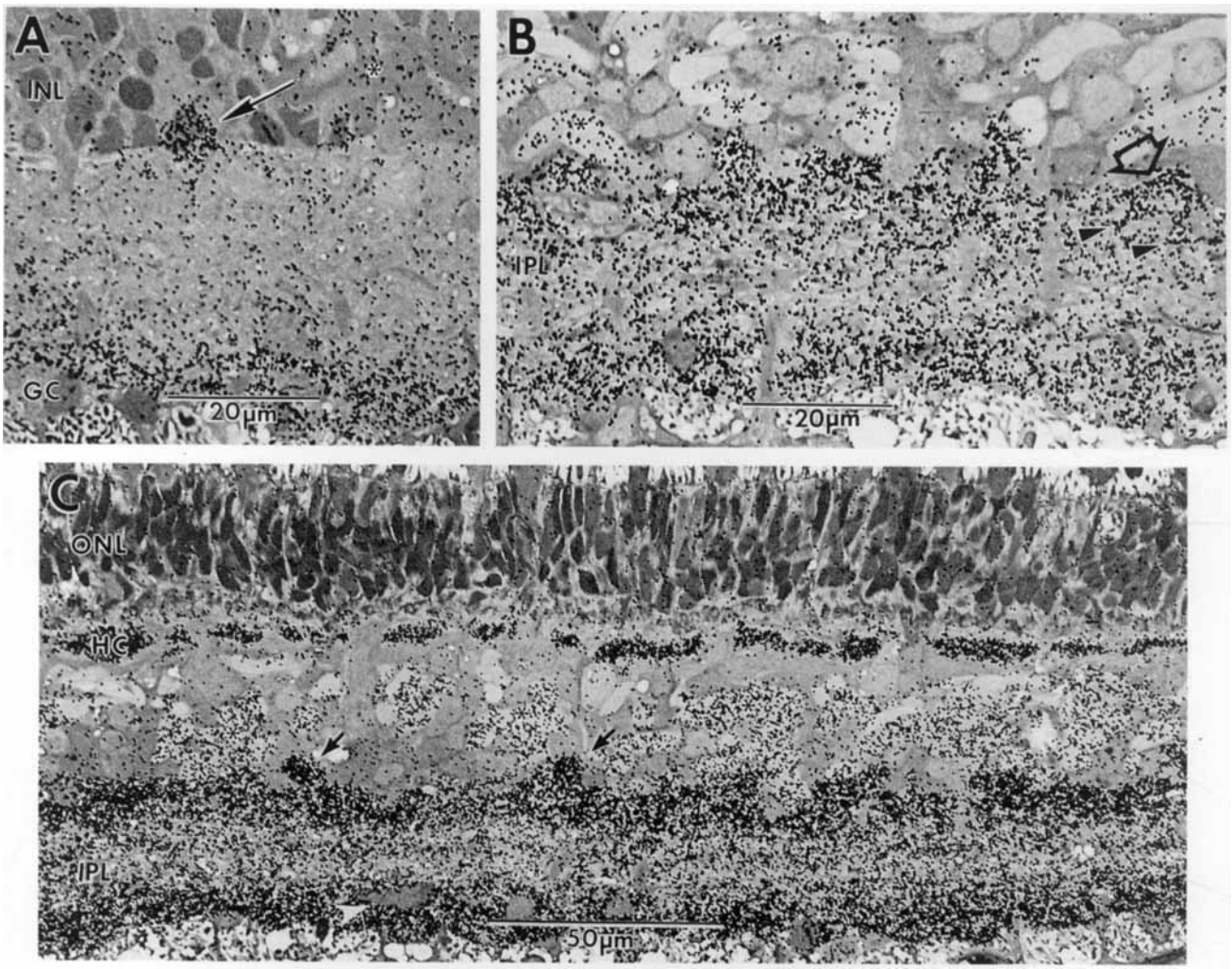

Fig. 1. ^{3}H-GABA uptake, light microscopic autoradiography. Comparison between a standard ^{3}H-GABA preparation (**A**) and ^{3}H-GABA + nipecotic acid preparations (**B,C**). All are 0.5 μm sections; A,C exposed for 4 weeks, B for 2 weeks. The arrow in A indicates a type Ab pyriform amacrine cell. A possible GABA-ergic transient amacrine cell and two of its dendrites are pointed out in B (large arrow and two dark arrowheads, respectively). Asterisks mark horizontal cell axon terminals. In C, a long view of a ^{3}H-GABA + nipecotic acid incubated sample, two cell bodies not obscured by the densely labeled band of the distal inner plexiform layer are indicated by arrows. Large terminals from type Mb, depolarizing mixed rod-cone bipolar cells are seen surrounded by grains in the proximal inner plexiform layer (white arrowhead).

Double-label data analysis

Standard sample analysis entailed following labeled profiles through serial sections within each grid, over consecutive grids where possible. Parlodion-coated slot grids allowed unobstructed viewing of numerous structures from section to section. In most cases, vertical or near-vertical views were selected for resectioning and double-label analysis. Vertical sections are advantageous in that they allow 1) clear mapping of the levels in the inner plexiform layer at which the individual ganglion cells ramify (see Figs. 3, 10) and 2) more serial sections per slot grid. The disadvantages of vertical sections stem from the relatively small portion of the HRP-labeled ganglion cell's dendritic arbor that each 40 or 60 μm section includes, approximately 5–10% for most of the individual ganglion cells sampled. In this study, depending on the individual ganglion cell or ganglion cell field sampled, the number of grids processed for EM autoradiography ranged from 30 to over 100 from each remounted thick section, with an average of seven or eight sections per grid.

The main object of this study has been to find unequivocal evidence of labeled amacrine cell input onto a given type of ganglion cell. To make a confident judgement, certain requirements had to be satisfied for each double-labeled synapse: 1) good overall tissue preservation; 2) clearly recognizable, well-oriented synapses; 3) pervasive postsynaptic HRP reaction product; and 4) significant presynaptic silver grain localization. Conventional synapses are recognized by a widened gap or "cleft" between the associated profiles, with vesicles aggregated along the presynaptic side and filamentous densifications on both sides. Even if the synaptic cleft is slightly oblique, these features are readily apparent. It will be assumed that such synapses represent sites of a physiological interaction between pre- and postsynaptic en-

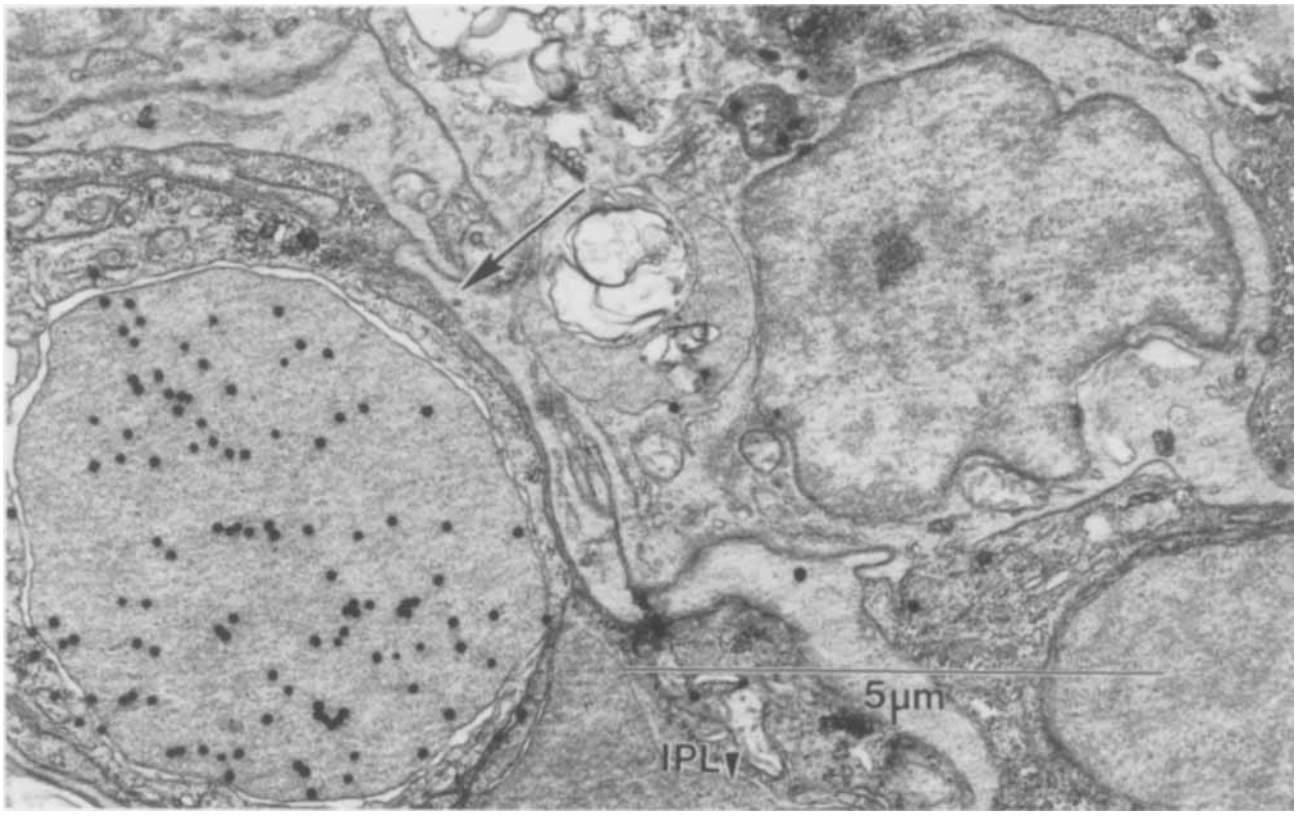

Fig. 2. ^{3}H-GABA + nipecotic acid, EM autoradiography. Signal to noise ratio. A detail from one of the inner nuclear layer regions analyzed. The grain density ratio of labeled (arrow) to unlabeled cell bodies, in these preparations, ranged from 17:1 to 19:1. The inner plexiform layer border (IPL, arrowhead) is indicated for orientation.

tities. Only solidly HRP-labeled ganglion cell processes have been included in the double-label analysis. The dense cytoplasmic flocculence, excluded from the mitochondria and most cisternae (Muller and Marc, '84), is quite characteristic and easily distinguishable under most circumstances. For characterizing significant presynaptic label, we relied on established statistical criteria for ultrastructural grain localization (Kelly and Weitsch-Dick, '78), where thresholds of three or four grains/μm^2 were calculated for central nervous tissue with a grain density ratio of 5:1 between labeled and unlabeled profiles. Data presented herein derive from specimens with grain density ratios of 17:1 or better for labeled vs. unlabeled areas. Our double-label analysis adopts a stringent standard of four grains per terminal in each of at least two serial sections, increasing the confidence level considerably. An important consideration in distinguishing autoradiographically labeled structures is the amount of "grain spread" expected for a particular preparation. Lateral grain displacement is primarily dependent on the thicknesses of the section and emulsion. For 70–80 nm sections and emulsion thickness of 70–100 nm, the predicted half-distance is 150–200 nm (Salpeter et al., '78); thus the distance from the terminal predicted to encompass about 90% of the localized grains would be about 500 nm (0.5 μm). In the labeled terminals presented here, silver grains are discretely localized well within those boundaries.

RESULTS

GABA-ergic inputs

High-affinity uptake, autoradiography. With relatively short incubations, moderate exposure times and concentrations in the micromolar range, GABA uptake is selective for H1 horizontal cells and their axon terminals, distally, and a population of large, pyriform amacrine cells (type Ab), with their labeled dendrites confined to the proximal 20% (L80–100) of the inner plexiform layer (Marc et al., '78, '88; Marc, '80, '82, '86, '89; Fig. 1A). Thus a major advantage of the standard incubation is selectivity for the type Ab pyriform amacrine cells and their monostratified arbor, allowing circuitry analysis of an individual cell type. However, immunocytochemical work (Ball '87; Ball and Brandon, '86; Marc, '86; Marc et al., '88; Yazulla et al., '86), labeling for GABA-like and GAD-like immunoreactivity, and ^{3}H-muscimol binding studies (Yazulla, '81), have given evidence that there are additional types of GABA-ergic amacrine cell in goldfish. It became apparent that there was likely to be a high density of GABA-ergic terminals throughout the inner plexiform layer, not only the proximal 20%. It has been suggested that in fishes (Marc, '86; '89; Marc et al., '88) and turtles (Tachibana and Kaneko, '84) the concentrations of high-affinity uptake sites, in both the outer plexiform and the inner plexiform layers, constitute spatial buff-

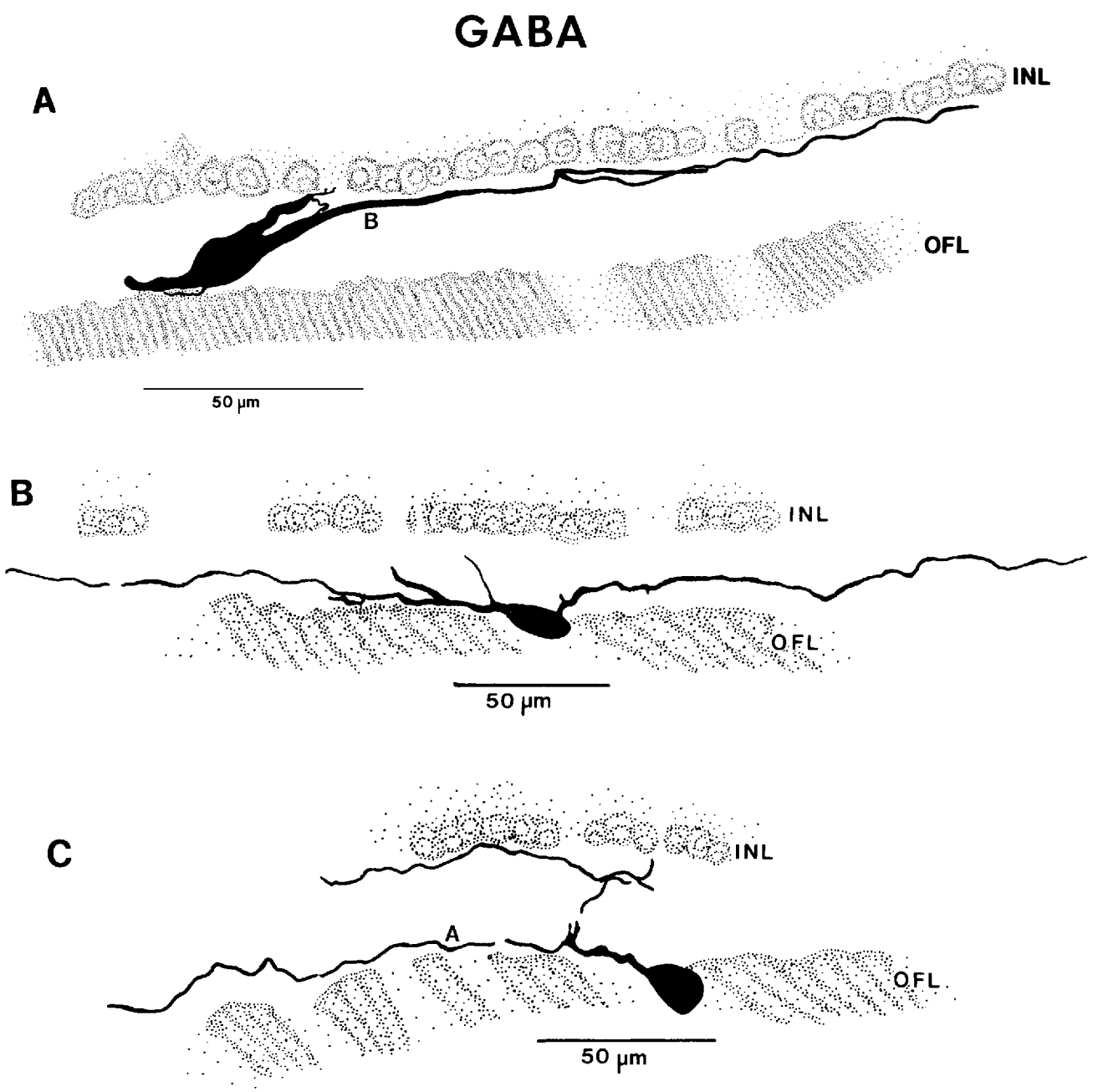

Fig. 3. Camera lucida drawings of HRP-labeled ganglion cells found to receive GABA-ergic inputs. **A:** A large ganglion cell, drawn from a 60 μm section, whose fusiform cell body is displaced to the inner plexiform layer. The dendritic arbor appears confined to sublayer 1, adjacent to the amacrine cells. Smaller letter B is the approximate location of the double-labeled synapse pictured in Figure 4B. This cell was drawn from a sample incubated in ^{3}H-GABA + nipecotic acid. Ganglion cells in B and C were drawn from standard ^{3}H-GABA-incubated preparations. **B:** A large ganglion cell drawn from a 40 μm section, apparently monostratified in sublamina b, that was found to receive GABA-ergic inputs from a type Ab pyriform amacrine cell dendrite in sublayer 5 (adjacent to the ganglion cell layer). **C:** A medium-sized ganglion cell, bistratified to the proximal and distal borders of the inner plexiform layer, drawn from a 40 μm section. The smaller letter A approximates the location of the double-labeled synapse pictured in Figure 4A. The inner nuclear layer (INL) and optic fiber layer (OFL) are indicated.

Fig. 4. Double-labeled synapses. GABA-ergic inputs onto selected individual ganglion cells. Asterisks mark the HRP-labeled dendritic profiles throughout; the double-labeled synapses are indicated by arrowheads. **A:** Two serial EM autoradiographs of GABA-ergic input from a type Ab pyriform amacrine cell onto the proximal dendrite of the bistratified ganglion cell pictured in Figure 3C. The arrowhead in A1 points to a GABA-ergic synapse onto an unlabeled profile of unknown origin. **B:** Four serial EM autoradiographs following a double-labeled synapse onto an off-center ganglion cell dendrite (Fig. 3A). The grains are small and well localized to the presynaptic profile. This is one of three GABA-ergic synapses found within 30 μm of the cell body; three others were found farther out.

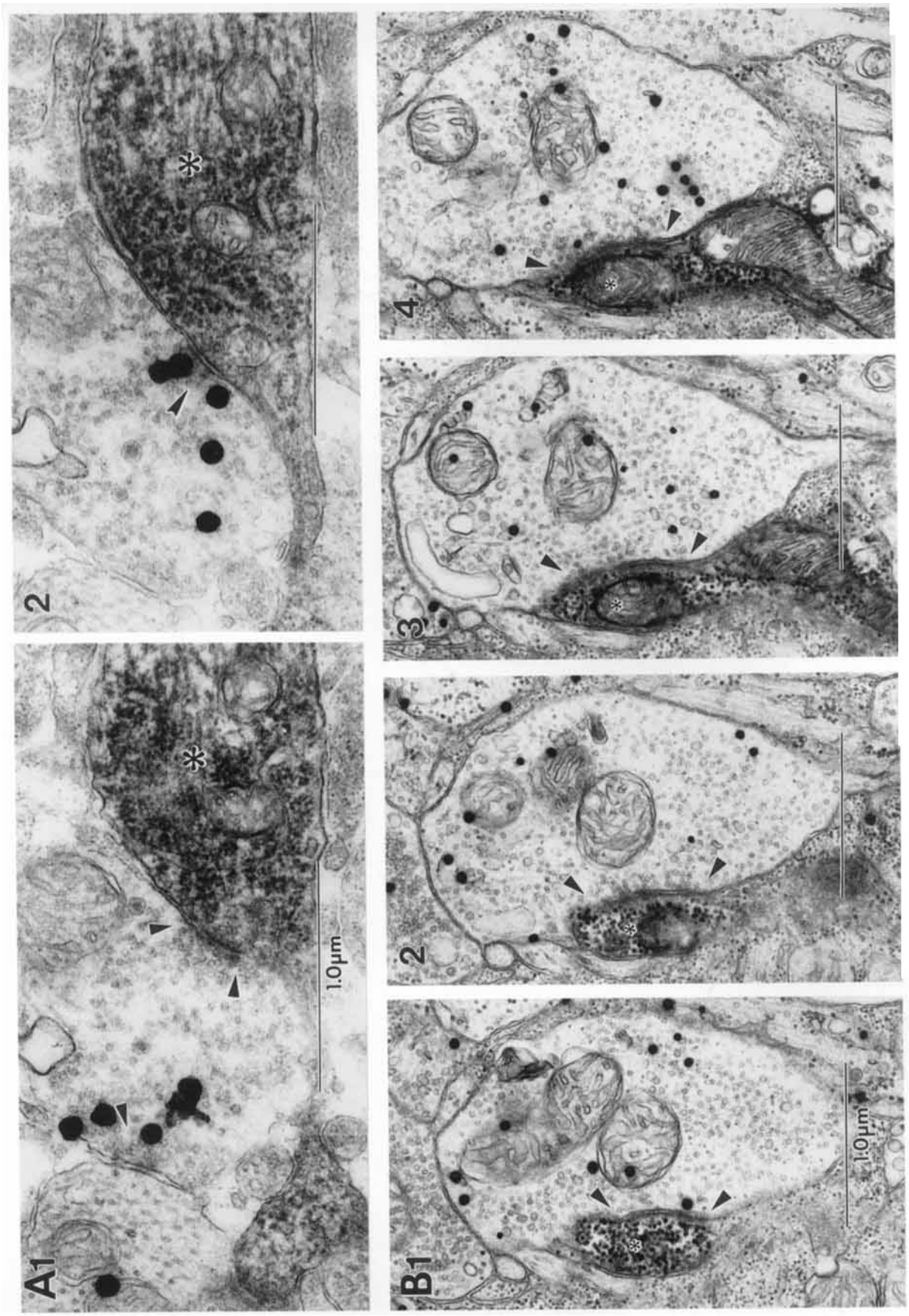

Figure 4

ers for GABA diffusion. During standard incubations this creates a sharp concentration gradient of ^{3}H-GABA, favoring the proximal border of the inner plexiform layer and the horizontal cell layer (Marc et al., '88; Marc, '89). The addition of millimolar concentrations of unlabeled GABA or nipecotic acid, as competitive inhibitors of GABA uptake, should reversibly occupy the uptake sites, allowing more ^{3}H-GABA to diffuse through the entire thickness of the retina. This modification allows a more comprehensive view of GABA-ergic stratification and the opportunity to label the full complement of GABA-ergic amacrine cells.

There is a dramatic difference between the label distributions after a standard ^{3}H-GABA incubation (Fig. 1A) and an incubation in ^{3}H-GABA with nipecotic acid added (Fig. 1B,C). Immediately noticeable is the dense stratum of label covering the distal 25% (L0–25) of the inner plexiform layer; in Figure 1C the band is nearly confluent, obscuring many of the labeled amacrine cells that lie adjacent to it. There also appear to be two discontinuous bands of label near L40 and L70 of the inner plexiform layer. Given the more extensive labeling of the ^{3}H-GABA + nipecotic acid preparations, it was necessary to gauge their overall specificity. Were the "newly" labeled cells clearly labeled? Was a large proportion of amacrine cells still clearly unlabeled? The grain density ratios of labeled to unlabeled cell bodies (i.e., signal to noise ratio) in the inner nuclear layer for several separate ^{3}H-GABA + nipecotic acid preparations (see Fig. 2) ranged from 17:1 to 19:1. This is well above the 5:1 ratio standard used by previous investigators (Kelly and Weitsch-Dick, '78) as a basis for their three or four grains/μm^2terminal criterion for statistically significant label (see Materials and Methods).

Double label: Individual ganglion cells. All double-labeled synapses were followed in serial sections. Some individual ganglion cells receiving GABA-ergic input are shown in Figure 3, representative double-labeled synapses are presented in Figure 4, and the remaining synapses onto these cells are represented on the GABA summary histogram in Figure 14. From standard ^{3}H-GABA preparations, we selected isolated, solidly labeled ganglion cells whose arbors were exclusively confined to, or well represented in, the proximal inner plexiform layer. Figure 3B and C are camera lucida drawings of ganglion cells that received inputs from GABA-ergic type Ab pyriform amacrine cells. The ganglion cell in Figure 3B is monostratified in the proximal region of the inner plexiform layer (sublamina b) and is probably an on-center ganglion cell. The cell in Figure 3C, stratified along the proximal and distal borders of the inner plexiform layer, is likely to be an on/off ganglion cell. Figure 4A presents two serial EM autoradiographs of a double-labeled synapse, one of the GABA-ergic inputs onto the proximal branch of the ganglion cell illustrated in Figure 3C. ^{3}H-GABA incubation with 1 mM nipecotic acid added to the medium allowed investigation of GABA-ergic inputs onto ganglion cells that arborize distally in the inner plexiform layer. A probable off-center ganglion cell with its dendritic arbor in sublayer 1 (L0–20; Fig. 3A), received GABA-ergic synapses at six loci along the dendrites pictured in Figure 3A. An example is shown in Figure 4B.

Double label survey through the inner plexiform layer. To survey GABA-ergic synapses onto ganglion cell dendrites through the inner plexiform layer, regions were selected for EM autoradiographic analysis from ^{3}H-GABA + nipecotic acid incubations, where 30–40% of the ganglion cells were solidly filled. Double-labeled synapses from different levels of the inner plexiform layer are shown in Figure 5A–D; the distribution of these inputs is summarized in Figure 14. Figure 5E, a detail from Figure 1C, serves as a key to the location of the double-labeled synapses. Figure 5B and C are two examples within L0–20 of the inner plexiform layer, thus included in the GABA-ergic system's broad distal stratum. Figure 5A shows a double-labeled synapse near L70, and Figure 5D shows one at about L90, near the ganglion cell layer border. We also found GABA-ergic synapses from large-caliber (2.5 μm and 2.0 μm diameters, respectively) microtubule-filled dendrites onto labeled ganglion cell cross sections (Fig. 6A, two serial sections near L70 and 6B within L15–20). These distally and proximally located amacrine cell processes are indistinguishable and frequently observed. We believe they are from the same cell type. Based on correlative evidence from this and other studies (see Discussion) we propose that both GABA-ergic profiles are from a type of transient on/off amacrine cell, bistratified in sublayers 1 and 4. Figure 5C exemplifies common double-labeled interactions, found near L10–15, involving small, rounded GABA-ergic endings.

Inputs onto bipolar cells. The ^{3}H-GABA + nipecotic acid protocol revealed GABA-ergic inputs onto a variety of bipolar cell profiles in sublayer 1 (L0–20), several of which were probably type Ma mixed rod-cone bipolar cells (Figs. 6, 7). With standard ^{3}H-GABA incubations, it had been established that type Mb bipolar cells receive profuse inputs from the GABA-ergic type Ab pyriform amacrine cell and that type Mb bipolar cells also provide ribbon inputs (Marc et al., '78). However, the neurochemical vector for feedback to the off-center pathway had not been defined. Based on present evidence, it appears that the predominant feedback inputs to both on- and off-center pathways (through mixed rod-cone bipolar cells) are GABA-ergic. In Figure 6, a large, scalloped, type Ma bipolar cell terminal near L05 receives five GABA-ergic inputs. It appears as if all amacrine cell profiles surrounding this view of the bipolar cell terminal accumulated GABA. Figure 7 shows a bipolar cell terminal near L10 (probably type Ma) receiving input from three GABA-ergic profiles. There is also a synapse between two of the profiles synapsing onto the bipolar cell terminal. If they are from two different types of amacrine cell then, based on these circuits, two subclasses of GABA-ergic sustained type Aa amacrine cells are predicted. Other pairs of GABA-ergic profiles synapsing onto one another were observed near L10 of the inner plexiform layer.

Glycinergic inputs

General morphology. Our knowledge of the glycine system in the goldfish is largely based on high-affinity uptake and autoradiography (Marc and Lam, '81). The previously known classes of glycinergic neurons were 1) a heterogeneous population of small, predominantly pyriform amacrine cells and 2) a population of interplexiform cells, pre- and postsynaptic to horizontal cells in the outer plexiform layer, with descending processes that terminate in the inner plexiform layer. Recent immunocytochemical work (Studholme and Yazulla, '88) has begun to further distinguish morphological classes of glycinergic amacrine cell at the light microscopic level. The most common morphological type encountered in the goldfish appears to be a small, pyriform amacrine cell (Fig. 8A). The single descending process appears to begin ramifying near L10–20, with the primary dendrite sometimes extending further. Studholme and Yazulla ('88) described a similar cell arborizing in the mid-

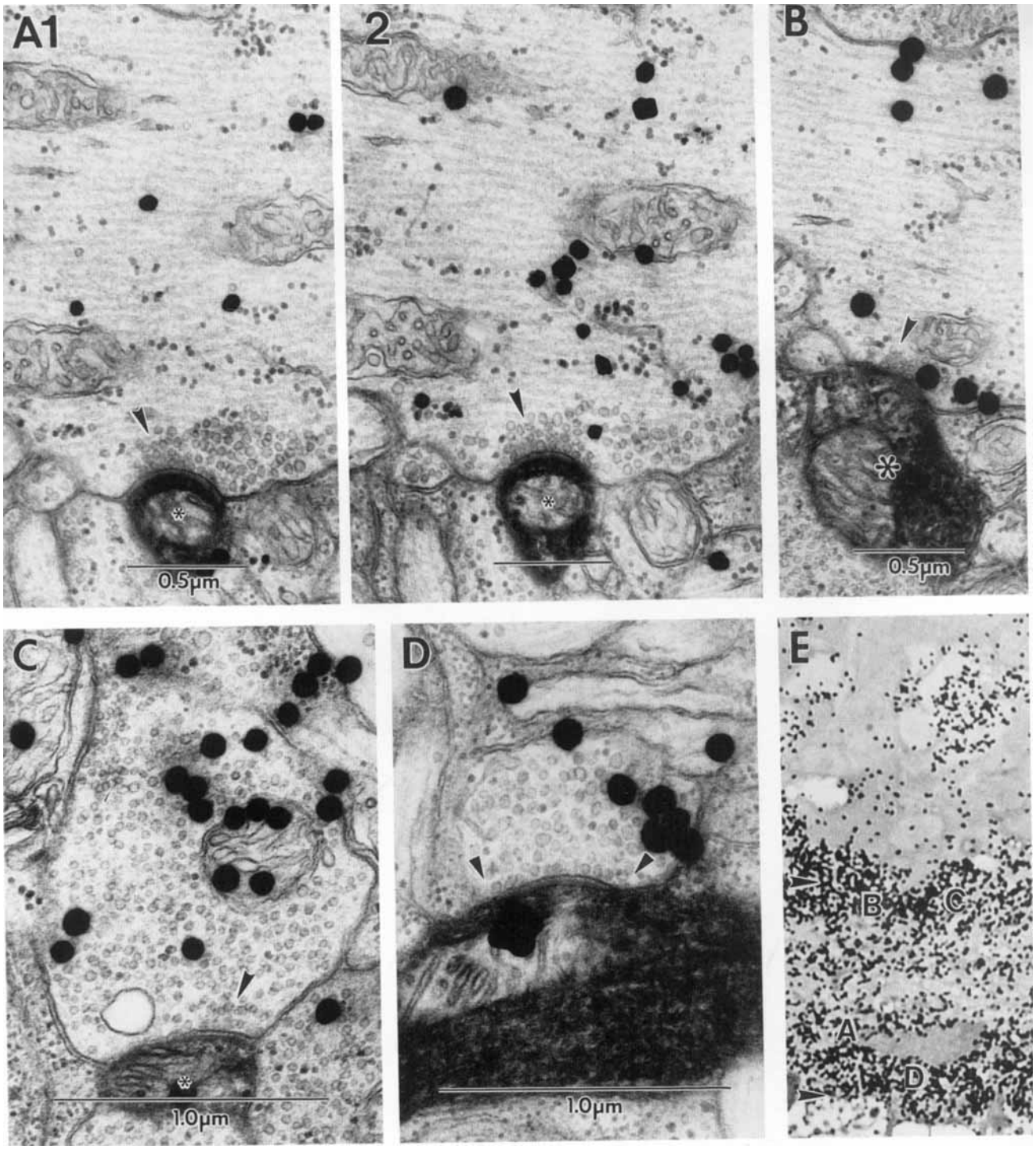

Fig. 5. Double-label survey through the inner plexiform layer. GABA-ergic inputs onto HRP-labeled ganglion cell dendrites. Retinal samples were incubated in ^{3}H-GABA + nipecotic acid, and regions were selected with 30–40% of the ganglion cells solidly labeled with HRP. **A:** Two serial sections of GABA-ergic input (arrowhead) onto a ganglion cell dendrite (asterisk) near L70 of the inner plexiform layer. **B:** GABA-ergic input onto a ganglion cell dendrite between L15 and L20. The GABA-ergic profile is similar to that pictured in A (see text). **C:** GABA-ergic input (arrowheads) onto a labeled ganglion cell profile near L10. **D:** Ganglion cell profile receiving GABAergic input (arrowheads) near L90. **E:** A detail of the light microscope autoradiograph in Figure 2C, as a key for the location of double-labeled synapses pictured in A–D. The inner plexiform layer borders are approximated by arrowheads.

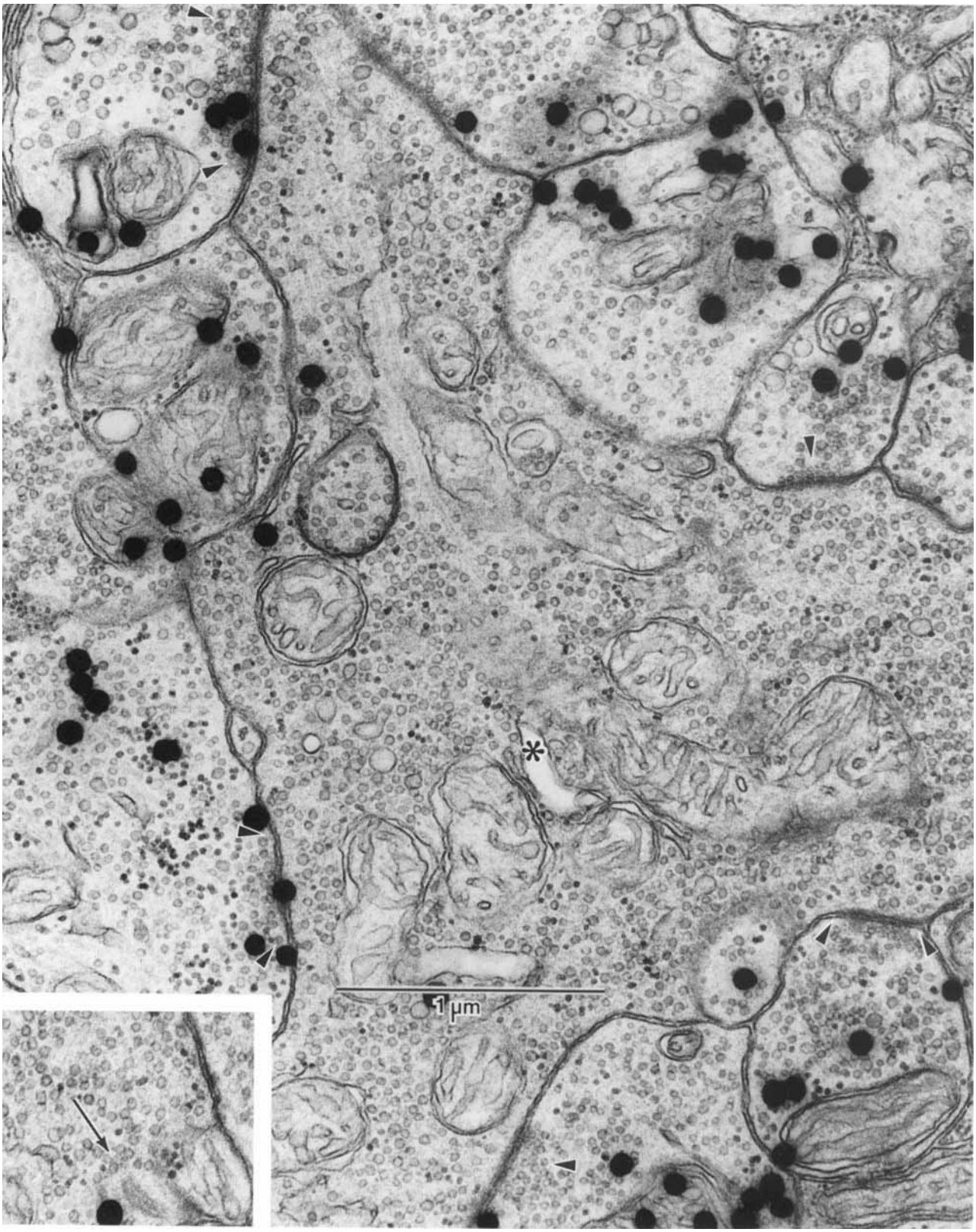

Fig. 6. GABA-ergic inputs onto a bipolar cell. A large, scalloped bipolar cell terminal (asterisk) near L05 of the inner plexiform layer, probably from a hyperpolarizing mixed rod-cone bipolar cell, receiving synaptic input (arrowheads) from five GABA-ergic profiles. **Inset:** at same magnification, a ribbon synapse (arrow) from approximately 2 µm to the right, out of the field of view.

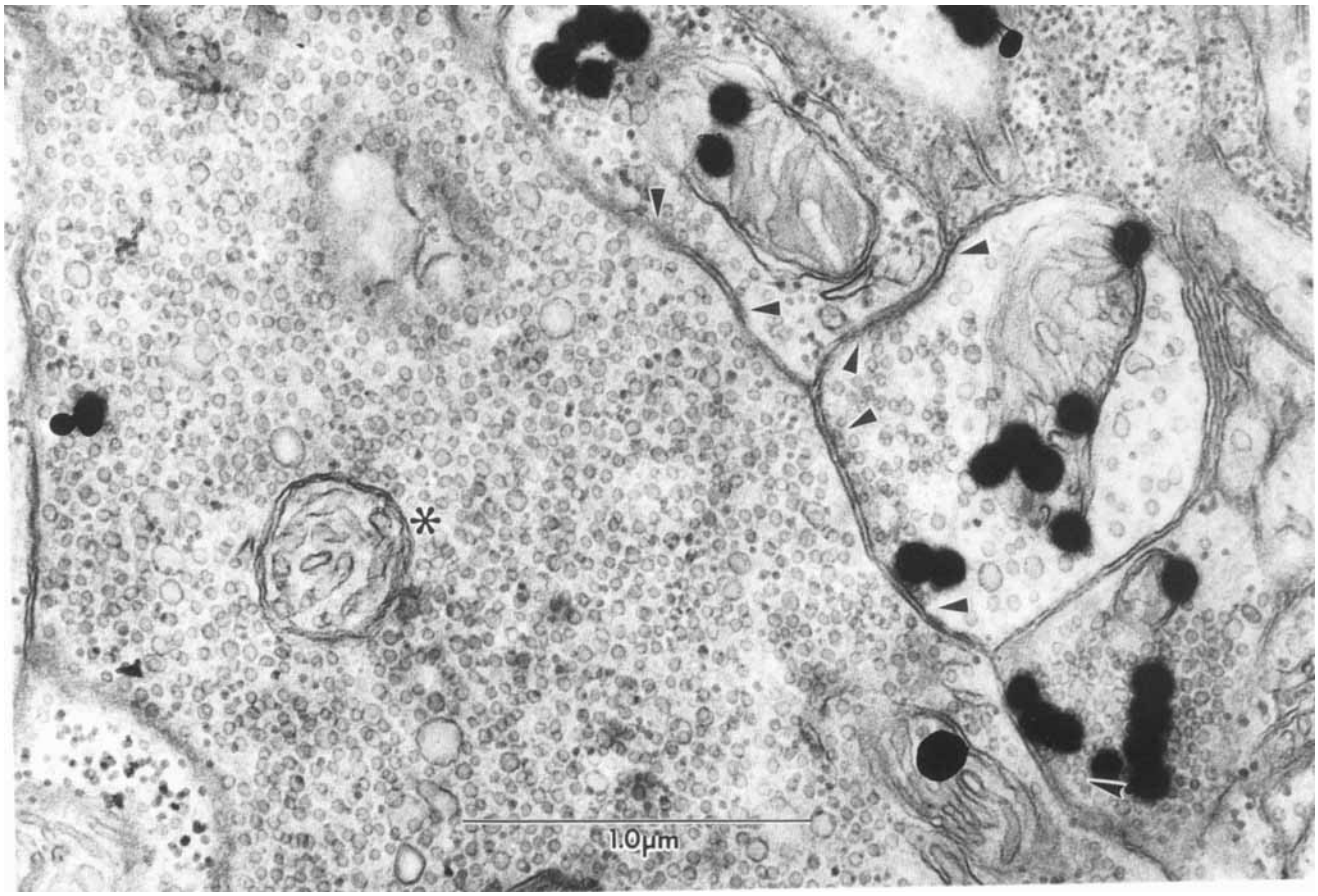

Fig. 7. Three GABA-labeled terminals synapsing (arrowheads) onto a bipolar cell terminal near L10 of the inner plexiform layer. There is also a synapse between two of the three GABA-ergic amacrine cell profiles that are synapsing on the bipolar cell terminal (asterisk).

dle of the inner plexiform layer. We also have evidence for a nonpyriform, multipolar subset of glycinergic amacrine cells (Fig. 8C). Whereas their lateral dendritic extensions may contribute significantly to the terminals of sublayer 1, their extent is difficult to determine. The glycinergic interplexiform cell is shown in Figure 8B, with a process ascending to the outer plexiform layer. The arbors of glycinergic amacrine and interplexiform cells in the inner plexiform layer are not completely distinguishable. However, there is now evidence from Golgi impregnation that glycinergic interplexiform cells arborize in sublayers 1 and 5, leaving the bulk of the inner plexiform layer labeling in sublayers 2, 3, and 4 due to glycinergic amacrine cells (Kalloniatis and Marc, '89).

The overall glcinergic label profile is punctate and clustered throughout the inner plexiform layer, concentrated in three discontinuous bands (strata) between L25 and L75 (probably entirely of amacrine cell origin). Glycinergic terminals are relatively sparse, both near the proximal border of the inner plexiform layer and in the outer plexiform layer. Thus, without the diffusion barriers observed with ^{3}H-GABA uptake, the spatial buffering of glycine uptake should be insignificant. As predicted, the addition of 1 mM unlabeled glycine to standard ^{3}H-glycine incubations has no qualitative effect (R.E. Marc, unpublished observations).

Light microscopic autoradiography of ^{3}H-glycine, as with ^{3}H-GABA + nipecotic acid preparations, shows a large proportion of cell bodies labeled in the inner nuclear layer, and labeled strata in both sublaminae a and b of the inner plexiform layer. To check our label specificity, we counted the grain density ratio between glycine-labeled cell bodies and unlabeled areas in the inner nuclear layer from low-power EM autoradiographs representing three different experiments (Fig. 9). The signal to noise ratio ranged from 29:1 to 32:1, clearly exceeding established criteria (Kelly and Weitsch-Dick, '78).

Double label: Individual ganglion cells. Four individual ganglion cells are shown, whose arbors were well isolated and onto which glycinergic synapses were followed in serial EM autoradiographs (Fig. 10A–D). The drawings in Figure 10A and D represent ganglion cells of similar somatic morphology, even though the cell in Figure 10A is displaced to the amacrine layer and the one in Figure 10D is in the ganglion cell layer. Both cells are large, spheroid, and multi-

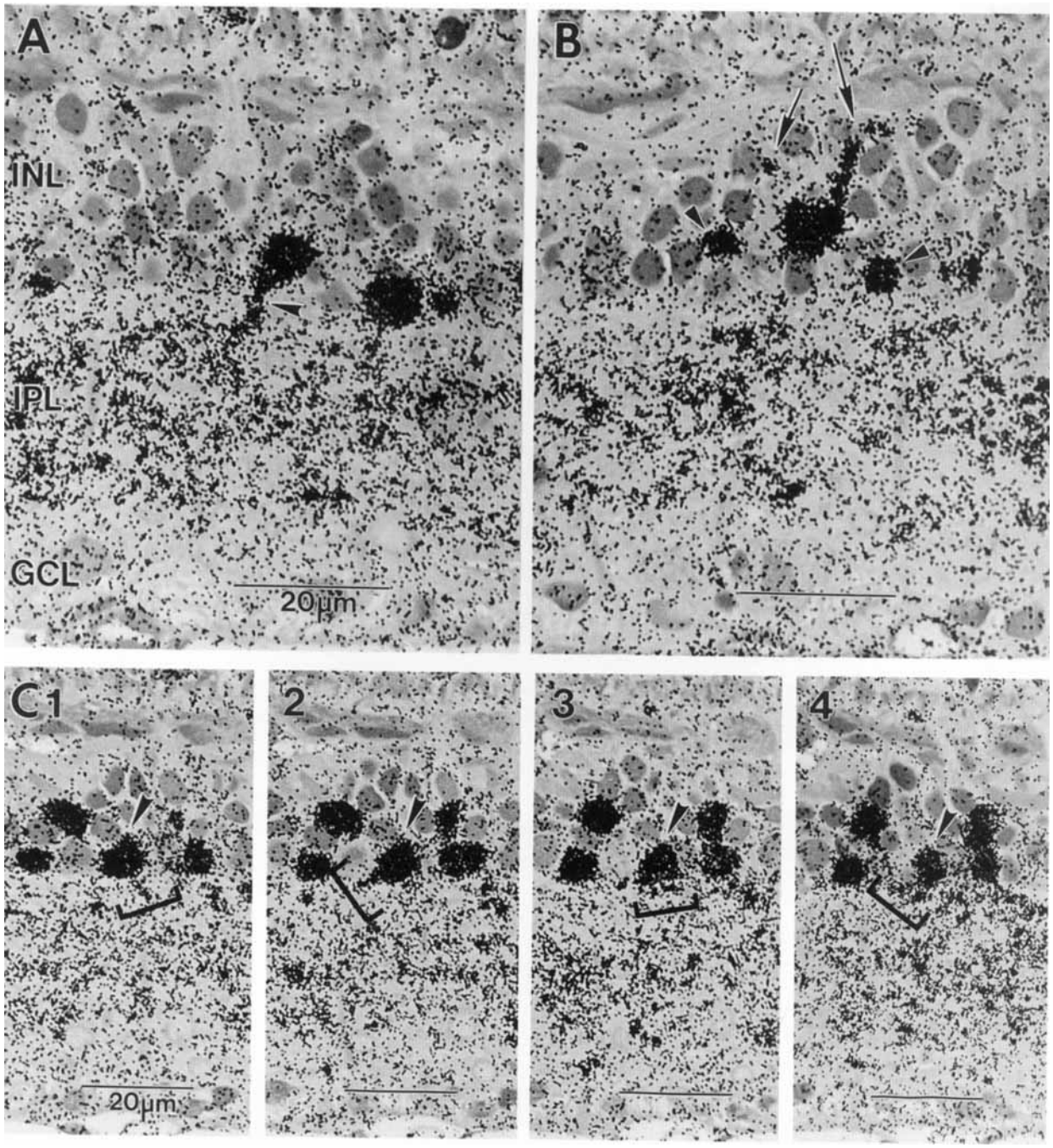

Fig. 8. Glycine uptake, light microscopic autoradiography. **A:** Pyriform glycinergic amacrine cell, arrowhead pointing to the descending primary dendrite. A detail from this view serves as a key to stratification in Figure 12. **B:** A glycinergic interplexiform cell with portions of two ascending processes indicated (arrows). Nearby amacrine cells are pointed out for comparison (arrowheads). **C:** Four serial sections depicting what may be one of a population of multipolar glycinergic amacrine cells (arrowheads). Dendrites appear to project from multiple sites on the cell body in different directions (brackets).

polar and have their dendritic arbors confined to L0–25 of the inner plexiform layer. Figure 11A presents two views of dendrites from the cell drawn in Figure 10A. Three serial sections (Fig. 11B) show glycinergic input onto a dendrite from one of the labeled profiles in Figure 11A. The silver grains are plentiful and well localized, and the pre- and postsynaptic densities and aggregated vesicles are clearly visible in each section. Also, as is often seen in large ganglion cell profiles, the HRP reaction product decorates the densely packed microtubules. Figure 10C is a camera lucida drawing from two consecutive 40 μm sections of a fairly large, pyriform ganglion cell stratified in the distal and middle levels

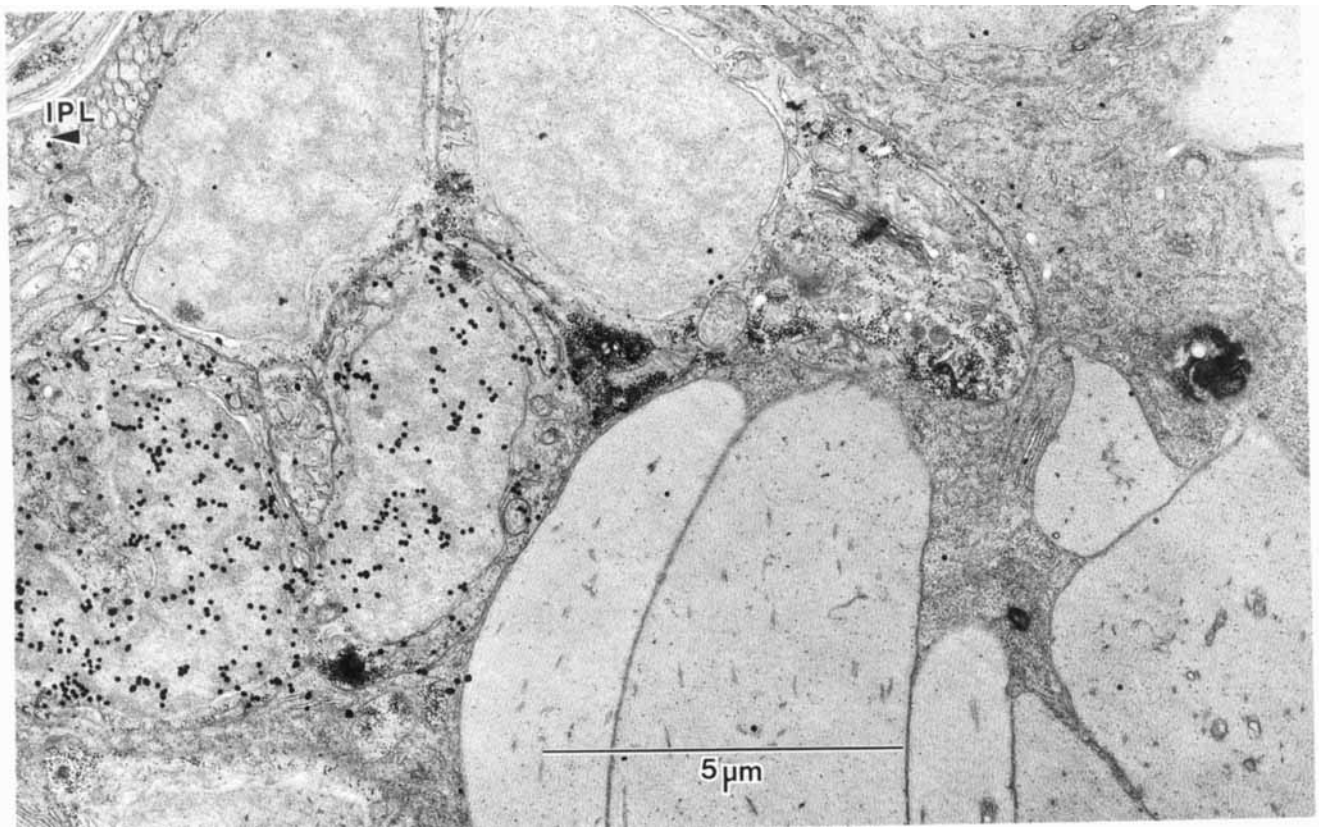

Fig. 9. ^{3}H-glycine uptake, EM autoradiography. Signal to noise ratio. A detail of an inner nuclear layer region, counted for grain density ratio between labeled cell bodies and unlabeled areas. Preparations analyzed had signal to noise ratios ranging from 29:1 to 32:1. For orientation, the location of the inner plexiform layer is indicated.

of the inner plexiform layer. Glycinergic synapses were found onto the labeled dendritic profiles in each stratum. The ganglion cell drawn in Figure 10B is large, fusiform, and displaced to the inner plexiform layer, with its broad, sparsely branched dendrites confined to sublayer 1. Figure 11C offers two serial views of a glycinergic input onto a labeled dendritic cross section from this probable off-center ganglion cell. It presents the same morphology as the ganglion cell pictured in Figure 3A, which was found to receive GABA-ergic inputs. Therefore, this appears to be one type of ganglion cell that receives both GABA-ergic and glycinergic input.

Double label survey through the inner plexiform layer. Glycinergic inputs were found onto labeled ganglion cell dendrites in each of the five sublayers. The most common regions for these synaptic contacts were near L30 and L90 of the inner plexiform layer (Fig. 12A–C). The double-labeled synapse in Figure 12A is at L85, one of three serial sections of a glycinergic input onto a slender ganglion cell dendrite. Figure 12B is one of two serial sections of glycinergic input from a glycogen-rich profile onto a small HRP-labeled ganglion cell cross section near L25. Although overall glycogen levels can fluctuate between preparations, certain glycine-labeled cells and profiles such as this contain a markedly high density. This is one instance of a labeled ganglion cell profile of 0.2 μm or less in diameter that receives input from a larger radiolabeled terminal. It is a good indicator of the resolution achievable with this technique. Only one glycinergic input was observed onto a bipolar cell in this study (Fig. 13). Given that mixed rod-cone bipolar cells in the proximal inner plexiform layer tend to be large and glycogen-rich, this may be a cone bipolar cell profile.

Double label: Data summary

The histograms in Figure 14 are a laminar account of 60 double-labeled synapses that clearly met our stringent label criteria. The open bars represent double-labeled synapses counted from retinal regions with 30–40% of the ganglion cells solidly filled, and the hatched bars represent synapses involving individual labeled ganglion cells, as illustrated in Figures 3, 4, 10, and 11. The hatched bar in the GABA histogram for the 80–100% interval represents data collected from standard ^{3}H-GABA incubated preparations (Figs. 1A, 3B,C, 4A). The remainder of the histogram bars in the GABA portion of Figure 16 represent double label data collected from preparations incubated in ^{3}H-GABA + nipecotic acid (Fig. 2B,C, 3, 5B, 6). The open bars in each histogram offer a preliminary survey of the overall distribution of GABA-ergic and glycinergic synapses onto ganglion cells. The pseudoautoradiographs (Marc, '86) allow comparison of the distributions of synapses in the inner plexiform layer

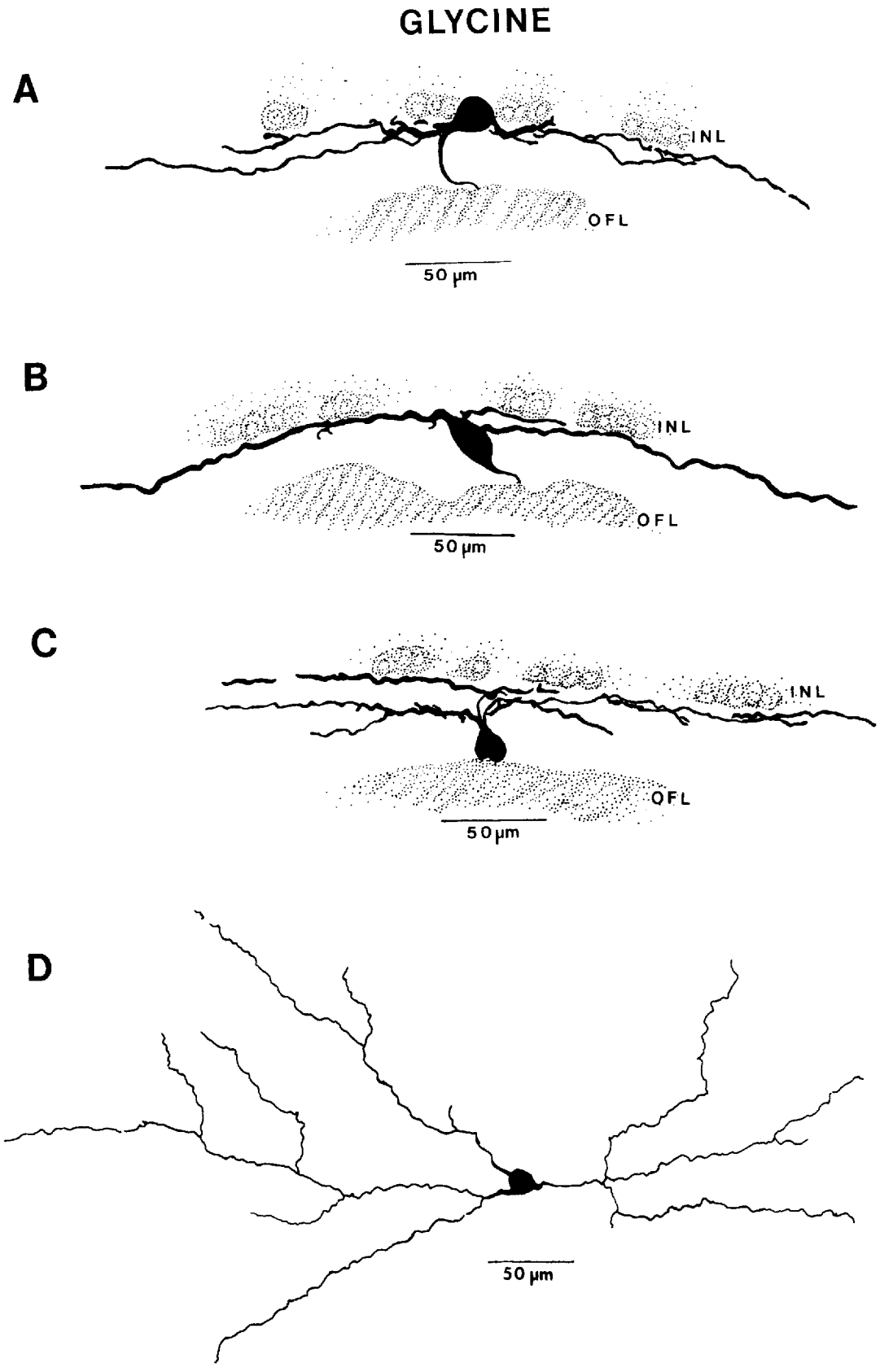

Figure 10

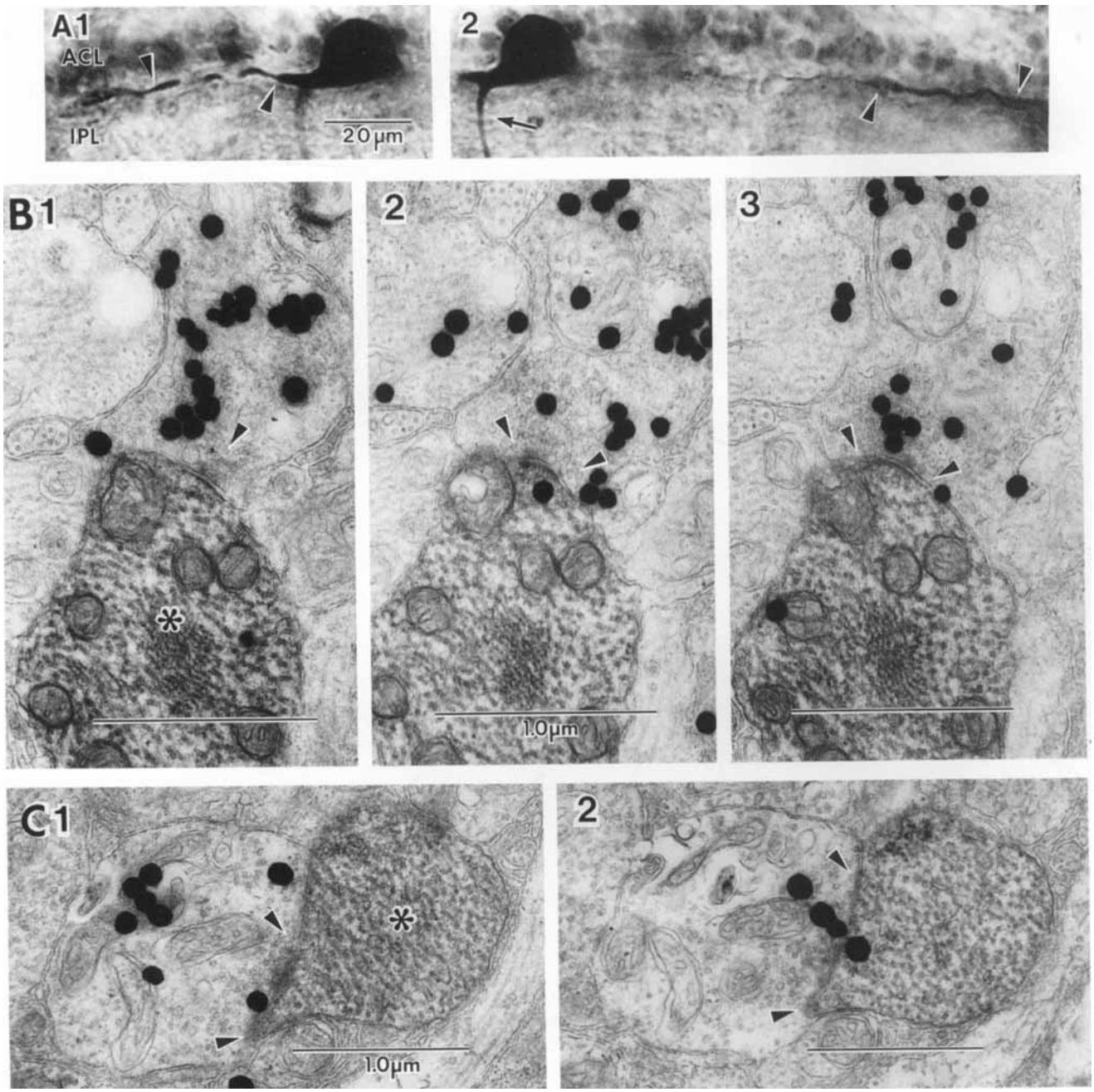

Fig. 11. Glycinergic inputs onto individual HRP-labeled ganglion cells. **A:** Light micrographs taken at two focal planes through the 40 μm section selected for EM autoradiographic analysis, from the cell drawn in Figure 10A. Opposing arrowheads trace the HRP-labeled dendrites, and an arrow points out the axon. **B:** Three serial EM autoradiographs following a synapse (arrowheads) onto an oblique cross section of one of the dendrites pictured in A (asterisk). **C:** Two serial views of a glycinergic synapse (arrowheads) onto a dendritic cross section from the cell illustrated in Figure 10B (asterisk). Although the synaptic cleft is somewhat oblique, the pre- and postsynaptic densities and aggregated synaptic vesicles are clearly visible.

Fig. 10. Camera lucida drawings of HRP-labeled ganglion cells found to receive glycinergic input. A, B, and D: Large cells, monostratified in the distal 25% of the inner plexiform layer. **D,** drawn horizontally from a 60 μm section, has its cell body in the ganglion cell layer. **A,** of similar morphology (drawn from three consecutive 40 μm sections), has its cell body displaced to the amacrine cell layer. **B** has a fusiform morphology, similar to the cell pictured in Figure 3A, with its cell body, displaced to the inner plexiform layer. **C,** drawn from two serial 40 μm sections, is apparently bistratified, ramifying in sublayers 1 and 3, receiving glycinergic input in both strata. All four cells are probably off-center ganglion cells.

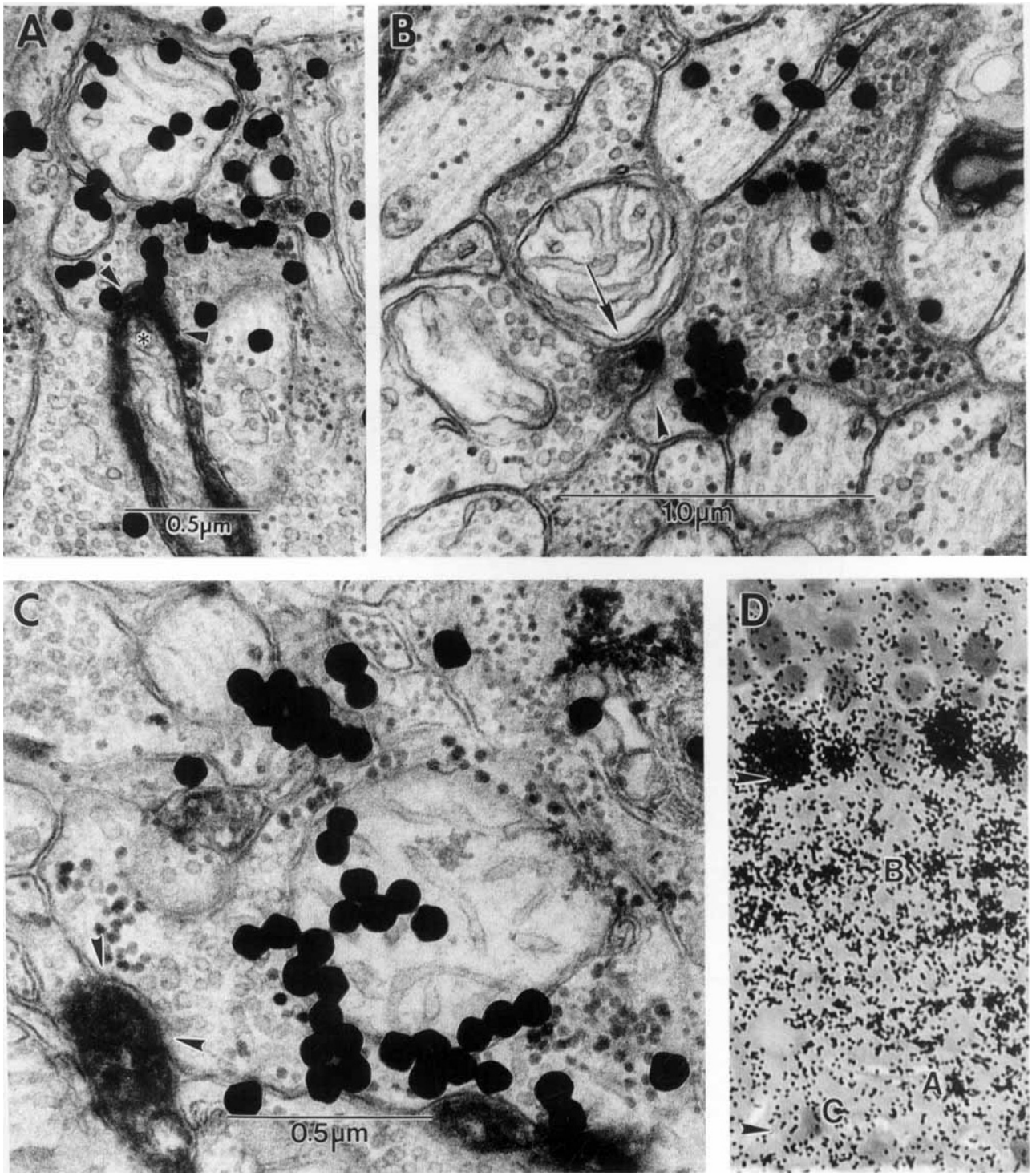

Fig. 12. Double label survey through the inner plexiform layer: Glycinergic inputs onto ganglion cells, regions selected where 30–40% of the ganglion cells were solidly labeled with HRP. **A:** One of three serial views of a slender ganglion cell dendrite (asterisk) receiving glycinergic input (arrowheads) near L85 of the inner plexiform layer. **B:** One of two serial sections of a glycinergic synapse (arrowhead) from a glycogen-rich terminal onto a small ganglion cell profile (arrow) near L25 of the inner plexiform layer. **C:** One of two glycinergic synapses (framed by arrowheads) from different glycinergic terminals onto the same HRP-labeled dendrite. **D:** A detail of the light microscope autoradiograph in Figure 8A as a key to the locations of double-labeled synapses in A–C. Approximate inner plexiform layer borders framed by arrowheads.

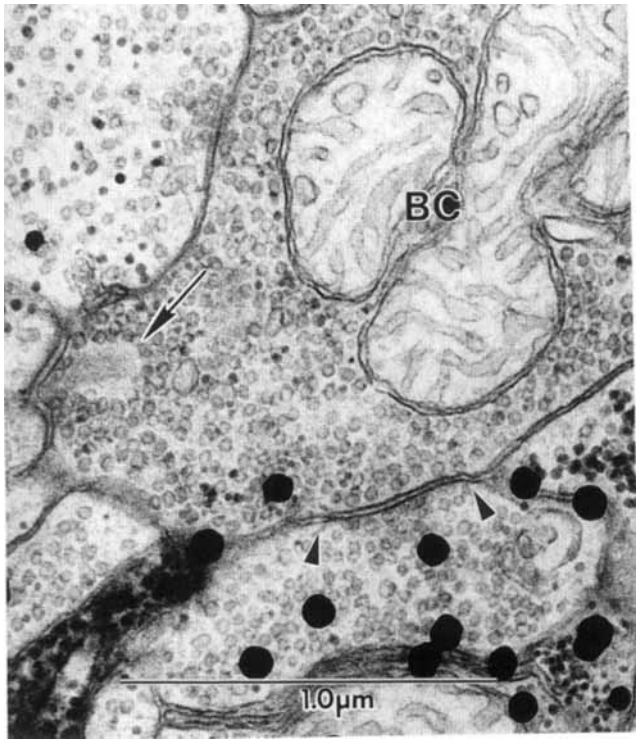

Fig. 13. A rare glycinergic input (arrowheads) onto a bipolar cell profile (BC). One of three serial sections, near L85. Note the synaptic ribbon (arrow).

with the major strata of GABA-ergic and glycinergic label. GABA-ergic and glycinergic synapses onto ganglion cells occur in every sublayer. The sample is not large enough to provide statistical significance about relative frequencies in particular sublayers, but there are trends that deserve further scrutiny. In the ^{3}H-GABA + nipecotic acid preparations, the first and fourth sublayers had the largest numbers of double-labeled synapses. In the ^{3}H-glycine preparations, the second and fifth sublayers registered the highest frequencies. ^{3}H-GABA + nipecotic acid experiments uncovered a dense band of label along the distal 25% of the inner plexiform layer (L0–25), and we have found that GABA-ergic inputs onto ganglion cells are prevalent where ^{3}H-GABA label is densest. For ^{3}H-glycine experiments, probable off-center ganglion cells were sampled, and glycinergic inputs onto individual ganglion cells did not allign with either of the two sublayers with apparent high frequencies of glycinergic inputs onto ganglion cells (sample bias). Sublayers two and five, specifically L25–35 and L85–90, included 65% of the glycinergic inputs onto ganglion cells surveyed through the inner plexiform layer. In fact, glycinergic inputs onto ganglion cells in sublayer five (L80–100) seem at least as frequent as GABA-ergic inputs. This is surprising, given the relatively low density of glycine label at that level. There may be an important segregation of targets for glycinergic neurons (see Discussion). Although GABA-ergic and glycinergic systems have a considerable number of outputs onto ganglion cells in the two distal sublayers, the GABA system dominates in sublayer 1 and the glycine system in sublayer 2.

DISCUSSION

Retrograde HRP transport

Injection of HRP into the optic nerve labels the retina heterogeneously. Some retinal regions have high densities of solidly labeled ganglion cells; other areas are more sparsely labeled. The regions with up to 40% of the ganglion cells solidly filled showed a broad morphological variety. Areas of the retinas where solidly labeled ganglion cells were relatively sparse proved useful in that the dendritic arbor of an HRP-labeled ganglion cell was more likely to be isolated. These regions appeared biased toward larger to medium-sized labeled cells. Individual labeled ganglion cells illustrated herein reflect that bias (Figs. 4, 12). Although we have noted the sizes, shapes, and locations of their cell bodies, individual labeled ganglion cells represented have been classified according to the apparent stratification of their dendrites in the inner plexiform layer.

Dye and current injection studies in teleosts (Naka, '77; Famiglietti et al., '77) indicate that on-center and off-center pathways in fishes are separate and parallel. Since we define on- and off-center regions of the inner plexiform layer by the locations of mixed rod-cone bipolar cell terminals (Ma [off-center] in sublayers 1 and 2, Mb [on-center] in sublayers 4 and 5), we predict that GABA-ergic and glycinergic synapses onto labeled ganglion cell profiles in sublayers 1 and 2 directly contribute to either off-center or on/off pathways, whereas similar synapses in sublayers 4 and 5 are directly influencing on or on/off pathways.

High-affinity uptake

Standard and modified approaches to high-affinity uptake and autoradiography have been employed in this study. Standard protocols for high-affinity uptake of ^{3}H-GABA and ^{3}H-glycine, as previously used in goldfish, showed characteristic labeling patterns, specific for unique populations of neurons (Marc et al., '78, '88; Marc, '80, '82, '85, '86, '89; Marc and Lam, '81; Marc et al., '88; this report). An alternative ^{3}H-GABA incubation protocol has been used to extend our understanding of GABA-ergic amacrine cell populations (Marc et al., '88; Marc, '89). Previous work had already established ultrastructurally that GABA-ergic type Ab amacrine cells reciprocally feedback onto depolarizing (on-center) bipolar cell terminals. This was based on the clear selectivity for type Ab pyriform amacrine cells by using standard ^{3}H-GABA preparations, with short incubations (Marc et al., '78, '88; Marc, '80, '82, '86). Incubations in ^{3}H-nipecotic acid, a competitive inhibitor of GABA uptake with similar affinity (Larsson et al., '80), show comparable selectivity (Ayoub and Lam, '84). Apparently, type Ab pyriform amacrine cells are the only GABA-ergic neurons, in fishes, that project to the proximal border of the inner plexiform layer. Using the modified ^{3}H-GABA uptake protocol, adding 1 mM nipecotic acid (Marc et al., '88; Marc, '89), a number of other questions could be explored. This approach labels nearly all GABA-ergic amacrine cells, as supported by the observations that 1) There is a 95–97% concordance between anti-GABA immunocytochemistry and ^{3}H-GABA + nipecotic acid labeling and 2) each method labels about 50–52% of all amacrine cells (Marc et al., '88; Marc, '89).

High-affinity uptake of ^{3}H-glycine labels two general classes of retinal neurons, amacrine cells and interplexiform cells, and shows evidence of labeled terminals throughout the inner plexiform layer (Marc and Lam, '81; this report) concentrated in three discontinuous bands between L25 and

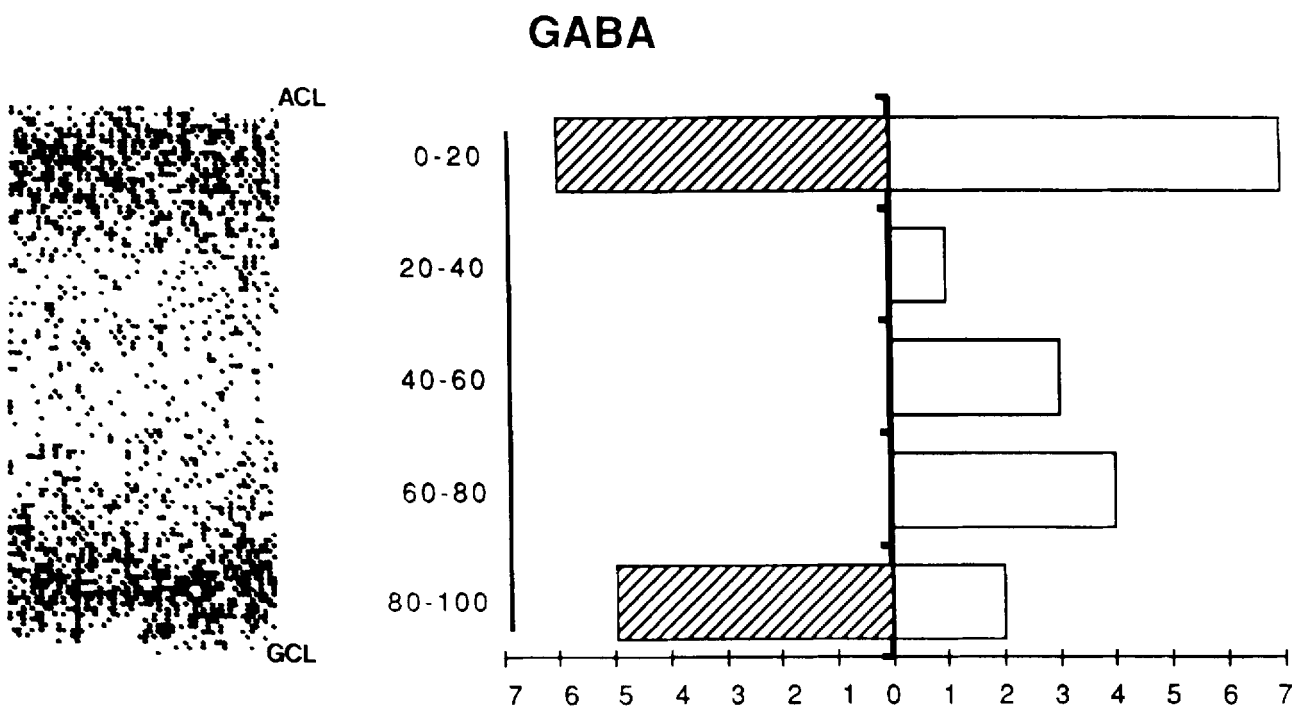

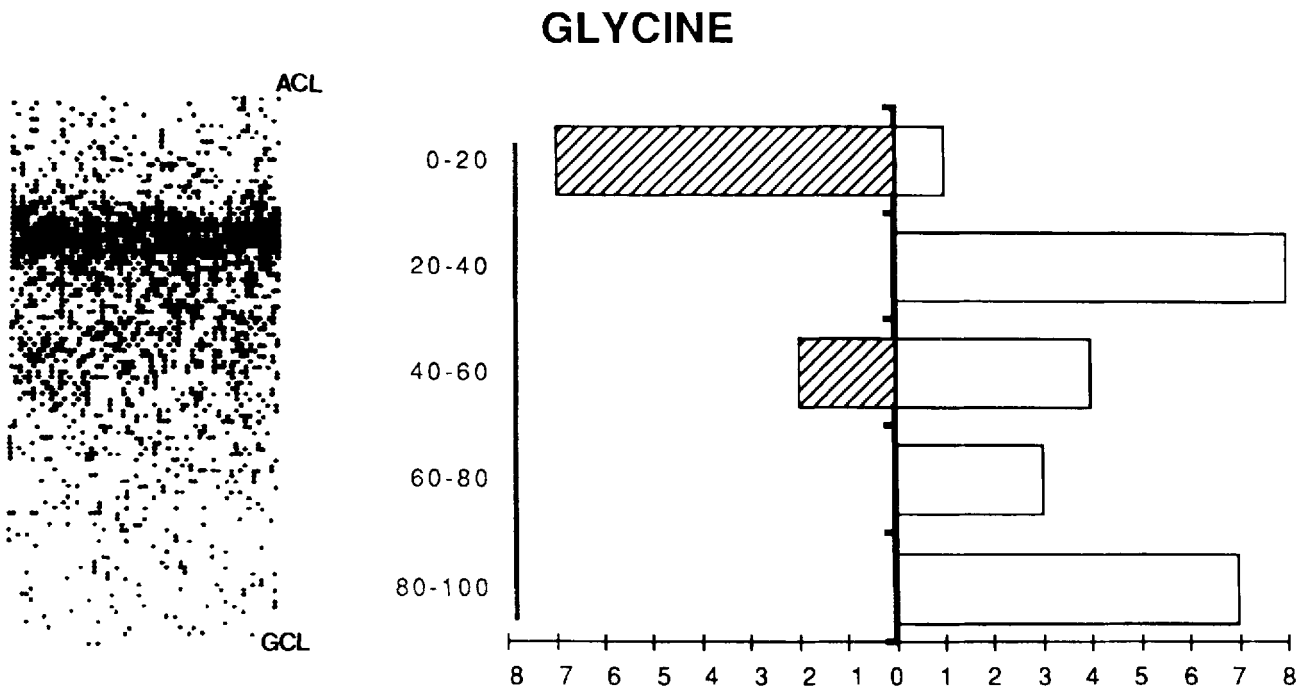

Fig. 14. Double label data summary. **Right:** Histograms. The ordinates indicate percent levels in the inner plexiform layer, bracketing the five sublayers. The abcissas tally unequivocal examples of double-labeled synapses within each sublayer. Hatched bars represent inputs onto individual ganglion cells; the open bars tally the double label surveys where 30–40% of the ganglion cells were solidly labeled with HRP. The hatched bar of the GABA histogram's 80–100% interval represents standard ^{3}H-GABA incubations, and the remainder of the GABA histogram represents ^{3}H-GABA + nipecotic acid incubated preparations. **Left:** Pseudoautoradiographs. The fields encompassing the light microscopic autoradiographs pictured in Figures 1C, 5E, 8A, and 12D were scanned densitometrically and converted to a dot matrix representation of the major strata for GABA-ergic and glycinergic terminals in the inner plexiform layer (see Marc, '86).

L75, in sublayers 2–4. Based on light microscopic autoradiography of serial sections, we propose at least two morphological types of glycinergic amacrine cell, one general population of small pyriform cells (Fig. 8A) and one type of apparently multipolar amacrine cell, with several dendrites projecting laterally from the cell body (Fig. 8C). Recently, Kalloniatis and Marc ('89) have obtained Golgi impregnations of glycinergic interplexiform cells that reveal that they arborize in sublayers 1 and 5 of the innerplexiform layer and not in sublayers 2, 3, or 4. In fact, the sublayer 5 dendrites appear to run just over the distal surfaces of the ganglion cells and may significantly contribute to the glycinergic synapses seen in that stratum.

EM autoradiographic analysis of GABA and glycine uptake in combination with retrograde HRP label of ganglion cells has led to some general conclusions. 1) Both GABA-ergic and glycinergic profiles are presynaptic to ganglion cell dendrites in each of the five sublayers. 2) There are ganglion cells that may receive direct synaptic input from both GABA-ergic and glycinergic neurons. 3) GABA-ergic amacrine cells contribute the predominant feedback input to both depolarizing and hyperpolarizing mixed rod-cone bipolar cells (i.e., on- and off-center pathways). Glycinergic synapses onto bipolar cells have been observed (Marc and Lam, '81; Studholme and Yazulla, '88; Fig. 13), but they are extremely rare.

The specificities of GABA-ergic and glycinergic markers for the neurons that use those neurotransmitters had been sources of some controversy (Marc, '86; Yazulla, '86; Marc et al., '88; Massey and Redburn, '87; Studholme and Yazulla, '88). It is now clear that the correspondence is excellent for GABA-ergic markers (Ball and Brandon, '86; Ball, '87; Marc et al., '88; Marc, '89). Furthermore, glycine uptake has a 0% overlap with GABA immunocytochemistry (Marc, '89), demonstrating complete separation of these systems (see also Marc, '85, '86).

DATA SUMMARY

GABA-ergic inputs

Figure 15A and B are schematic diagrams illustrating pathways to on, off, and on/off ganglion cells, with established and proposed interneurons GABA-ergic surround pathways. The H1 HC and the type Ab pyriform amacrine cell have been previously established as GABA-ergic (Marc et al., '78, '88; Yazulla et al., '87), a particular transient, on/off amacrine cell and certain type Aa amacrine cells are now proposed to be GABA-ergic.

In teleosts, large, fusiform transient amacrine cells, bistratified to sublayers 1 and 4, have been intracellularly recorded and dye injected by a number of investigators (Djamgoz et al., '85; Murakami and Shimoda, '77; Famiglietti et al., '77; Teranishi et al., '84, '85, '87) and found to be dye-coupled (Teranishi et al., '84). Ultrastructural evidence is provided herein that similarly bistratified GABA-ergic amacrine cells synapse onto ganglion cells in both their dendritic strata. Large caliber, nontapering dendrites near L10 and L70 were found in these double-label preparations to label with GABA, and we provide evidence for their inputs onto labeled ganglion cells in both strata (Fig. 5A,B). We encountered gap junctions on some of these profiles, but not unequivocally contacting homologous dendrites. GAD and GABA immunocytochemistry (Ball and Brandon, '86; Ball, '87; Marc et al., '88; Marc, '89) and both light and electron microscopic ^{3}H-GABA + nipecotic acid autoradiography reveal large, fairly common amacrine cells with distinct, 2–3 μm diameter, nontapering or mildly tapering dendrites arborizing in sublayers 1 and 4 (Marc et al., '88; Figs. 5A,B, 14). It seems just a matter of time before the above-described transient amacrine cell will be definitively established as GABA-ergic.

As Figure 15 illustrates, GABA-ergic type Aa amacrine cells synapse onto hyperpolarizing bipolar cells and off-center ganglion cells based on profuse GABA-ergic inputs onto type Ma bipolar cells in sublayer 1 (Marc, '89; Figs. 6, 7). Bipolar cells respond in a sustained manner to light, so it is assumed that amacrine cells synapsing onto bipolar cells are sustained amacrine cells. Several sustained-off amacrine cells have been recorded and dye injected (Teranishi et al., '85). Each was monostratified in sublamina a, but their morphologies varied from pyriform to fusiform. Finding profuse GABA-ergic type Aa feedback onto Ma bipolar cells is exciting because it means that GABA-ergic amacrine cells provide the predominant feedback for both on- and off-center pathways in goldfish. GABA-ergic inputs were also found onto the HRP-labeled probable off-center ganglion cell pictured in Figure 3A (see Fig. 4B), and the GABA-labeled amacrine cell profiles closely resembled the small rounded swellings seen synapsing onto Ma bipolar cells. GABA-ergic Aa amacrine cells have also been found to synapse onto other GABA-labeled profiles in sublayer 1 (Fig. 7). This may indicate multiple classes of GABA-ergic Aa amacrine cells. Synapses between putatively GABA-ergic amacrine cell dendrites have also been described in mammals (Vaughan et al., '81; Kolb and Nelson, '85; Mariani and Caserta, '86).

Figure 15 specifies the synaptic transfers of on- and off-center pathways, indicating whether the polarity of the postsynaptic response is conserved (+) or inverted (−). The on- and off-center visual pathways in vertebrates are distinguished from one another by a single sign inversion between the receptors and depolarizing bipolar cells (Slaughter and Miller, '81, '83; Miller and Slaughter, '85; Nawi and Copenhagen, '87). For the purposes of this discussion, all bipolar–ganglion cell interactions will be considered excitatory and sign-conserving (Naka, '77; Slaughter and Miller, '83; Massey and Redburn, '87).

The left diagram in Figure 15A represents the previously established (Marc et al., '78) and the right the newly proposed GABA-ergic surround inputs to on- and off-center pathways. Figure 15B outlines proposed sustained (left) and transient (right) GABA-ergic amacrine cell inputs onto (transient) on/off ganglion cells. Standard ^{3}H-GABA incubations select type Ab pyriform amacrine cells (Marc et al., '78) that reciprocally synapse with type Mb bipolar cells. In the right diagram in Figure 15A, an additional circuit contributes to the on pathway: GABA-ergic feed-forward on-center ganglion cells. Thus there are a minimum of three GABA-ergic surround inputs that converge on a single on-center ganglion cell: 1) H1 HC→cone feedback, 2) Ab AC→Mb BC feedback, and 3) Ab AC→on GC feed-forward. Samples incubated in ^{3}H-GABA + nipecotic acid allow a nearly complete assessment of GABA-ergic inputs to the off-center pathway. Direct inputs onto probable off-center ganglion cells arise from proposed GABA-ergic Aa amacrine cells. GABA-ergic Aa amacrine cells also synapse on Ma bipolar cells (see Figs. 6, 7), and many of these inputs are reciprocal (Marc et al., '88; Marc, '89). The path from GABA-ergic H1 horizontal cells to off-center ganglion cells is net sign-inverting (one − synapse in the chain). Thus

GABA

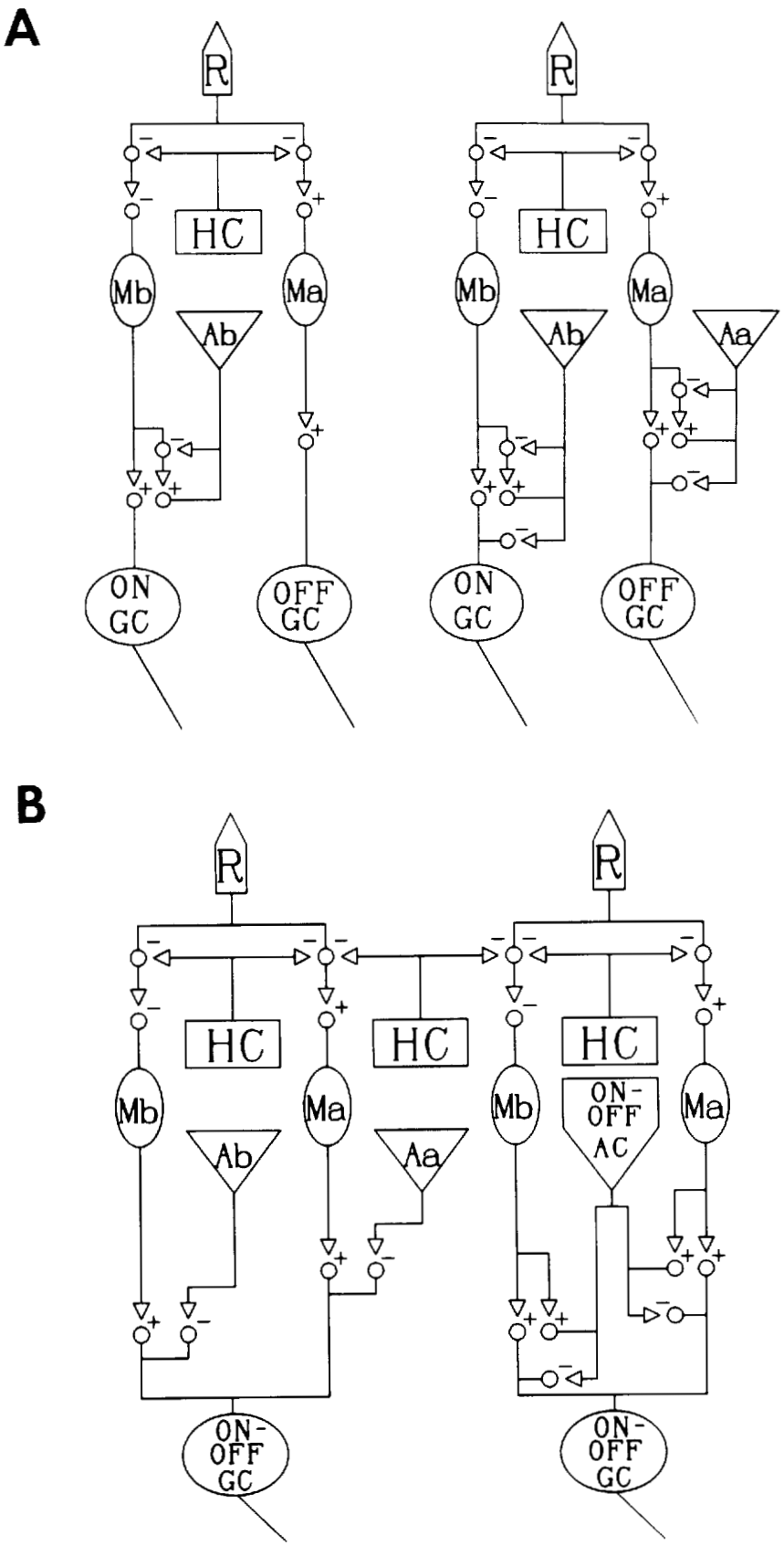

Figure 15

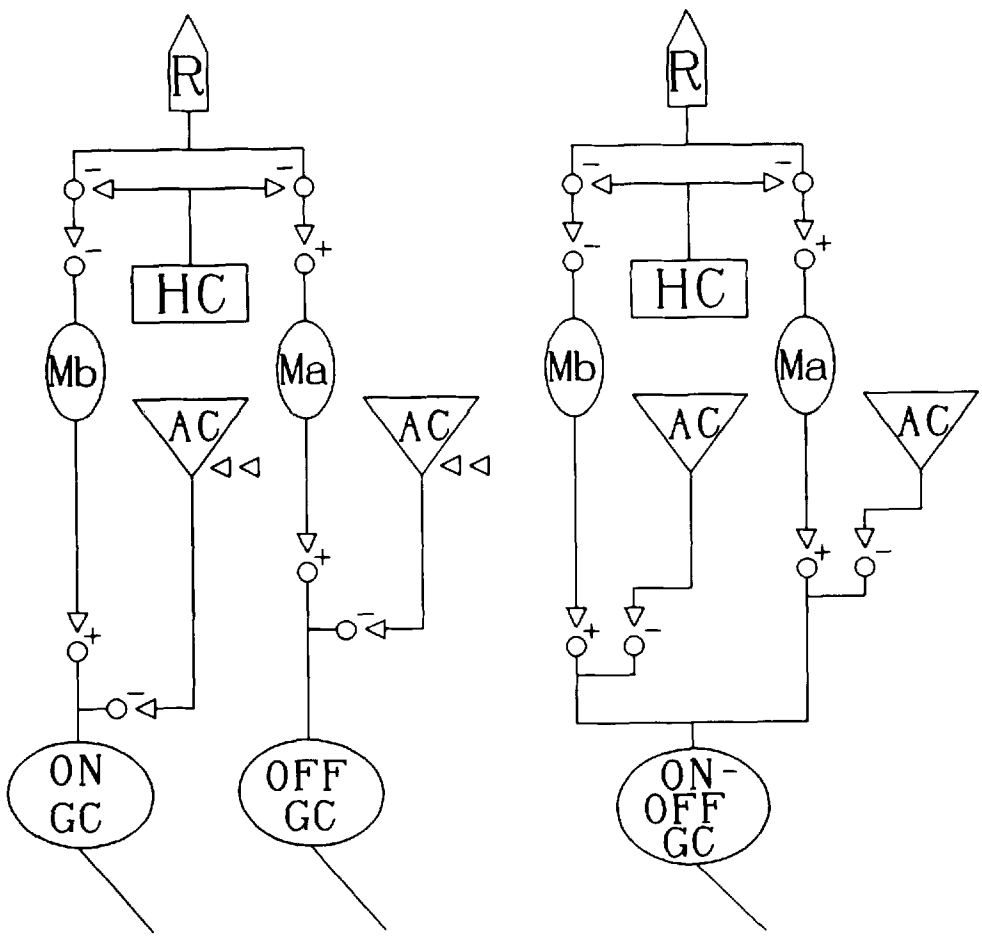

Fig. 16. Schematic diagram of glycinergic pathways in the goldfish retina. The two major categories of glycinergic neurons in the goldfish are a heterogeneous population of small amacrine cells and an interplexiform cell that receives input from horizontal cells in the outer plexiform layer and sends terminals to the inner plexiform layer. They are collectively abbreviated AC for this diagram. Further study has begun to subdivide the amacrine cells (see also Studholme and Yazulla, '88). **Left:** Direct evidence for glycinergic inputs to off-center ganglion cells is illustrated in Figures 10 and 11. Glycinergic inputs to on-center ganglion cells is suggested by data in Figure 12A,C and summarized in Figure 14 (see text). The double arrowheads with the glycinergic amacrine cells symbolize that the predominant inputs to glycinergic amacrine cells are from other amacrine cells. **Right:** Glycinergic inputs onto on/off ganglion cells are suggested by frequent glycinergic synapses onto HRP-labeled ganglion cells in both sublaminae a and b. Recent data suggest that many glycinergic synapses in sublayer 5 come from glycinergic interplexiform cells (Kalloniatis and Marc, '89).

Fig. 15. GABA-ergic inputs to on-center, off-center, and on/off pathways. A + indicates a sign-conserving and a − indicates a sign-inverting synapse. **A: Left:** Previously established circuits in the goldfish inner plexiform layer. Employing standard high-affinity uptake of ^{3}H-GABA, it had been found that GABA-ergic Ab pyriform amacrine cells and type Mb bipolar cells interact reciprocally in a feedback circuit (Marc et al., '78). **Right:** New circuits in the goldfish inner plexiform layer. Double label with standard ^{3}H-GABA uptake revealed GABA-ergic inputs from Ab pyriform amacrine cells onto probable on-center ganglion cells: A feed-forward circuit. Data from ^{3}H-GABA + nipecotic acid preparations reveal GABA-ergic feed-forward to probable off-center ganglion cells by type Aa amacrine cells and reciprocal GABA-ergic feedback onto probable hyperpolarizing mixed rod-cone bipolar cells (see also Marc, '89). **B:** Pathways to on/off ganglion cells. **Left:** Inputs from probable sustained GABA-ergic amacrine cells. Figures 3C and 4A illustrate type Ab pyriform, sustained on-center amacrine cell synapses onto the proximal branches of bistratified probable on/off ganglion cells. The direct influence of sustained off-center, GABA-ergic Aa amacrine cells on on/off ganglion cells is speculative, based on the large proportion of GABA-labeled terminals that synapsed onto HRP-labeled ganglion cells in sublayer 1. **Right:** Proposed direct GABA-ergic transient, on/off amacrine cell inputs onto on/off ganglion cells in both sublaminae.

hyperpolarization of H1 horizontal cells by light should effect a depolarization in the off-center ganglion cells, consistent with the electrophysiological results of Naka ('77) for catfish. Since the net paths between GABA-ergic Aa amacrine cells and both Ma bipolar cells and off-center ganglion cells is sign-inverting (one – synapse), the off pathway has three ultimately sign-inverting surround fields converging on ganglion cells. As we learn more about the combinations of inputs onto the various GABA-ergic neurons, we can better predict their spatial, temporal, and chromatic contributions to the opponent-surround.

Transient on/off ganglion cells respond both to light onset and to light offset with a short burst of action potentials and often multistratified, in both sublaminae a and b (Famiglietti et al., '77; Murakami and Shimoda, '77; Teranishi et al., '84, '85, '87; Djamgoz et al., '85; Djamgoz, '86; Djamgoz and Wagner, '87). They presumedly receive inputs from transient amacrine cells, which, in turn, are believed to be driven by depolarizing and hyperpolarizing bipolar cells (Toyoda et al., '73; Famiglietti et al., '77; Frumkies et al., '81; Toyoda and Fujimoto, '84; Miller and Slaughter, '85; Djamgoz, '86; Kujiraoka et al., '88). Recent evidence, including data presented here, indicates that sustained amacrine cells influence transient ganglion cells as well (Belgum et al., '83). Figure 15B is a set of circuit diagrams outlining the proposed influences on the transient on/off ganglion cells by sustained GABA-ergic amacrine cells (left diagram) and transient GABA-ergic amacrine cells (right diagram). The left diagram is simplified, in that the amacrine cell reciprocal feedback onto Ma and Mb bipolar cells, as illustrated in Figure 15A, is implied. It is expected that the three GABA-ergic surround inputs to on- and off-center pathways are present for on/off pathways, as well. Figures 3C and 4A depict synaptic input from GABA-ergic Ab pyriform amacrine cells (sustained on-center) to the proximal branch of a bistratified ganglion cell, likely to be an on/off ganglion cell. The proposed Aa (sustained off-center) influence on the on/off ganglion cell is based merely on the large proportion of GABA-ergic terminals surveyed that synapsed onto HRP-labeled ganglion cells of a variety of dendritic morphologies in sublayer 1 (L0–20) of the inner plexiform layer. Evidence is presented in Figures 1B and 5A,B that a bistratified (probable transient) amacrine cell is GABA-ergic and synapses onto ganglion cells in both sublayers 1 and 4. Thus a fourth GABA-ergic opponent-surround pathway is proposed. The hyperpolarizing and depolarizing bipolar cells presumedly converge on GABA-ergic transient amacrine cells, which subsequently synapse on transient on/off ganglion cells.

Glycinergic inputs

The combined arbor of the glycinergic amacrine cells and interplexiform cells reaches all levels of the inner plexiform layer, although three bands in sublayers 2–4 are often apparent (Marc, '86; Fig. 9, 12D). Ultrastructurally, glycinergic terminals are often seen as clusters of profiles, frequently running along side each other, making no apparent contacts with one another. Figure 12C shows a ganglion cell dendrite with input from one of two adjacent glycinergic endings. Although adjacent glycinergic profiles could be distinguished by relative glycogen content or slight differences in electron density or vesicle concentration, we could not claim different cells of origin.

Figure 16 schematizes the mixed rod-red cone pathways in the goldfish retina and describes our limited knowledge of how surrounds are affected by the glycine system. The predominant inputs to the glycinergic system of the inner plexiform layer are from other, nonglycinergic amacrine cells. Direct glycinergic input occurs onto a variety of probable off-center ganglion cells (Figs. 10, 11, and 14), whereas direct glycinergic inputs to on-center ganglion cells are suggested by data presented in Figure 12A,B and the glycine summary presented in Figure 14. With about 30% of the double-labeled synapses occurring in sublayer 5 (L80–100), it is likely that some involve on-center ganglion cells (although we cannot rule out that they may all be on/off ganglion cells). However, sublayer 5 is a major terminator site for glycinergic interplexiform cells (Kalloniatis and Marc, '89). The discordance between the frequency of glycinergic inputs to ganglion cells (high in sublayer 5; see Fig. 14) and the density of glycinergic terminals (low in sublayer 5; see Marc and Lam, '81; Marc, '86; this report) suggests that a significant proportion of ganglion cell inputs from ^{3}H-glycine-labeled profiles could be from glycinergic interplexiform cells (see also Rayborn et al., '81). Given that the glycinergic system synapses onto ganglion cells in every sublayer, one or a variety of glycinergic neurons could also synapse onto transient on/off ganglion cells. Furthermore, there are no clear clues to whether glycinergic inputs are from sustained or transient cells; both possibilities exist (see Marc and Lam, '81). Although there is evidence of glycinergic inhibitory effects on on-center, off-center, and on/off ganglion cells (Negishi et al., '78), we still lack correlative physiology for any morphologically defined glycinergic neuron in fishes. With these uncertainties, and our general lack of understanding of inputs to glycinergic neurons in the inner plexiform layer, we cannot at this point speculate on their light-evoked effects on on-center and off-center pathways. Further morphological work (in progress) and more detailed physiological study should help resolve these issues.

ACKNOWLEDGMENTS

This research was supported by NIH grant EY 02576.

LITERATURE CITED

Adams, J.C. (1981) Heavy metal intensification of DAB-based HRP reaction product. J. Histochem. Cytochem. *29*:775.

Ames, A. III, and F.B. Nesbett (1981) In vitro retina as an experimental model of the central nervous system. J. Neurochem. *37*:867–871.

Ayoub, G.S., and D.M.K. Lam (1984) The release of γ-aminobutyric acid from horizontal cells of the goldfish (*Carassius auratus*) retina. J. Physiol. *355*:191–214.

Ball, A.K. (1987) Immunocytochemical and autoradiographic localization of GABAergic neurons in the goldfish retina. J. Comp. Neurol. *255*:317–325.

Ball, A.K., and C. Brandon (1986) Localization of ^{3}H-GABA, -muscimol and -glycine in goldfish retinas stained for glutamate decarboxylase. J. Neurosci. *6*:1621–1627.

Belgum, J.H., D.R. Dvorak, and J.S. McReynolds (1983) Sustained and transient synaptic inputs to on-off ganglion cells in the mudpuppy retina. J. Physiol. *340*:599–610.

Bouteille, M. (1976) The "LIGOP" method for routine ultrastructural autoradiography: A combination of single grid coating, gold latensification and phenidon development. J. Microsc. Biol. Cell *27*:121–128.

Brandon, C. (1985) Retinal GABA neurons: Localization in vertebrate species using an anti-serum to rabbit brain brain glutamate decarboxylase. Brain Res. *344*:286–295.

Cohen, B., and G.L. Fain (1988) GABA and glycine channels in isolated ganglion cells from the goldfish retina. Invest. Ophthalmol. Vis. Sci. Suppl. *29*:104.

Djamgoz, M.B.A. (1986) Common features of light-evoked amacrine cell responses in vertebrate retina. Neurosci. Lett. *71*:187–191.

Djamgoz, M.B.A., J.E.G. Downing, E. Wagner, H.-J. Wagner, and I. Zeutzius (1985) Functional organization of amacrine cells in the teleost retina. In A. Gallego (ed): Neurocircuitry of the Retina, A Cajal Memorial. New York: Elsevier, pp. 188–204.

Djamgoz, M.B.A., W.K. Stell, C.-A. Chin, and D.M.K. Lam (1981) An opiate system in the goldfish retina. Nature *292*:620–623.

Djamgoz, M.B.A., and H.-J. Wagner (1987) Intracellular staining of retinal neurons: Applications to studies of functional organization. In N. Osborne (ed): Progress in Retinal Research Vol 6. Oxford: Pergamon, pp. 85–150.

Famiglietti, E.V. Jr., A. Kaneko, and M. Tachibana (1977) Neuronal architecture of on and off pathways to ganglion cells in the carp retina. Science *198*:1268–1269.

Famiglietti, E.V. Jr., and H. Kolb (1976) Structural basis for on and off-center responses in retinal ganglion cells. Science *194*:193–195.

Frumkies, T.E., R.F. Miller, M. Slaughter, and R.F. Dacheux (1981) Physiological and pharmacological basis of GABA and glycine action on neurons of the mudpuppy retina. III. Amacrine-mediated inhibitory influences on ganglion cell receptive field organization: A model. J. Neurophysiol. *45*:783–805.

Glickman, R.D., A.R. Adolph, and J.E. Dowling (1982) Innerplexiform circuits in the carp retina: Effects of cholinergic agonists, GABA, and substance P on the ganglion cells. Brain Res. *234*:81–99.

Ishida, A.T., and B. Cohen (1988) GABA-activated whole cell currents in isolated retinal ganglion cells. J. Neurophysiol. *60*:381–396.

Ishida, A.T., W.K. Stell, and D.O. Lightfoot (1980) Rod and cone inputs to bipolar cells in goldfish retina. J. Comp. Neurol. *191*:315–335.

Kalloniatis, M., and R.E. Marc (1989) Golgi impregnated interplexiform cells in the goldfish retina. Invest. Ophthalmol. Vis. Sci. Suppl. (in press).

Kaneko, A., E.V. Famiglietti Jr., and M. Tachibana (1979) Physiological and morphological identification of signal pathways in the carp retina. In M. Otsula (ed): Neurobiology of Chemical Transmission. New York: Wiley, pp. 235–251.

Kaneko, A., Y. Nishimura, N. Tachibana, M. Tauchi, and K. Shamai (1981) Physiological and morphological studies of signal pathways in the carp retina. Vision Res. *21*:1519–1526.

Kaneko, A., Y. Nishimura, M. Tauchi, and K. Shamai (1980) Distribution of afferent synapses along on-center bipolar cells axons in the carp retina. Biomed. Res. *1*:345–348.

Kelly, J.S. and F. Weitsch-Dick (1978) Critical evaluation of the use of radioautography as a tool in the localization of amino acids in the mammalian nervous system. In F. Fonnum (ed): Amino Acids as Chemical Transmitters. New York: Plenum, pp. 102–121.

Kolb, H. (1982) The morphology of the bipolar cells, amacrine cells and ganglion cells in the retina of the turtle *Pseudemys scripta elegans*. Phil. Trans. R. Soc. London [Biol.] *298*:355–393.

Kolb, H., and R. Nelson (1984) Neuronal architecture of the cat retina. In N. Osborne (ed): Progress in retinal Research Vol. 3. Oxford: Pergamon, pp. 22–60.

Kolb, H., and R. Nelson (1985) Functional neurocircuitry of amacrine cells in the cat retina. In A. Gallego (ed): Neurocircuitry of the Retina, a Cajal Memorial. New York: Elsevier, pp. 215–232.

Kujiraoka, T., T. Saito, and J.-I. Toyoda (1988) Analysis of synaptic inputs to on-off amacrine cells of the carp retina. J. Gen. Physiol. *92*:475–487.

Lam, D.M.K., and B.-B. Li, Y.-Y.T. Su, and C.B. Watt (1985) The signature hypothesis: Co-localizations of neuroactive substances as anatomical probes for circuitry analysis. Vision Res. *25*:1353–1364.

Lam, D.M.K., and L. Steinman (1971) The uptake of [γ-^{3}H]aminobutyric acid in the goldfish retina. Proc. Nat. Acad. Sci. *68*:2777–2781.

Lam, D.M.K., Y.Y.T. Su, L. Swain, R.E. Marc, C. Brandon, and J.-Y. Wu (1979) Immunocytochemical localization of L-glutamic acid decarboxylase in the goldfish retina. Nature *278*:565–567.

Larsson, O.M., P. Krogsgaard-Larson, and A. Shoesboe (1980) High affinity uptake of (RS)-nipecotic acid in astrocytes cultured from mouse brain. Comparison with GABA transport. J. Neurochem. *34*:970–977.

Madtes, P. Jr., and D. Redburn (1985) Metabolism of [^{3}H]nipecotic acid in the rabbit retina. J. Neurochem. *44*:1520–1523.

Marc, R.E. (1980) Retinal colour channels and their neurotransmitters. In G. Verriest (ed): Colour Deficiencies V. London: Adam Hilger, pp. 15–29.

Marc, R.E. (1982) Spatial organization of neurochemically classified interneurons of the goldfish retina: I. Local patterns. Vision Res. *22*:589–608.

Marc, R.E. (1985) The role of glycine in retinal circuitry. In W.W. Morgan (ed): Retinal Transmitters and Modulators: Models for the Brain. Boca Raton, FL: CRC Press, Vol. 1, pp. 119–158.

Marc, R.E. (1986) Neurochemical stratification of the inner plexiform layer of the vertebrate retina. Vision Res. *26*:223–238.

Marc, R.E. (1989) The anatomy of multiple GABAergic and glycinergic pathways in the inner plexiform layer of the goldfish retina. In R. Weiler and N. Osborne (eds): The Neurobiology of the Inner Retina: Nato/AS Series. Berlin: Springer-Verlag, pp. 53–64.

Marc, R.E., and D.M.K. Lam (1981) Glycinergic pathways in the goldfish retina. J. Neurosci. *1*:152–165.

Marc, R.E., and W.-L.S. Liu (1984) Horizontal cells synapses onto glycine-accumulating interplexiform cells. Nature *311*:266–269.

Marc, R.E., W.-L.S. Liu, and J.F. Muller (1988) Multiple GABA-mediated surround channels in goldfish retina. Invest. Ophthalmol. Vis. Sci. Suppl. *29*:272.

Marc, R.E., W.K. Stell, D. Bok, and D.M.K. Lam (1978) GABAergic pathways in the goldfish retina. J. Comp. Neurol. *182*:221–246.

Mariani, A.P., and M.T. Caserta (1986) Electron microscopy of glutamate decarboxylase (GAD) immunoreactivity in the inner plexiform layer of the rhesus monkey retina. J. Neurocytol. *15*:645–655.

Massey, S.C., and D.A. Redburn (1987) Transmitter circuits in the vertebrate retina. Prog. Neurobiol. *28*:55–96.

Miller, R.F. (1988) Are single neurons both excitatory and inhibitory. Nature *336*:517–518.

Miller, R.F., and R.F. Dacheux (1976) Synaptic organization and ionic basis of on and off channels in mudpuppy retina. III. A model of ganglion cell receptive field organization based on chloride free experiments. J. Gen. Physiol. *67*:679–690.

Muller, J.F., and R.E. Marc (1984) Three distinct morphological classes of receptors in fish olfactory organs. J. Comp. Neurol. *222*:482–495.

Muller, J.F., and R.E. Marc (1988) GABAergic and glycinergic pathways in the inner plexiform layer of the goldfish retina. Invest. Ophthalmol. Vis Sci. Suppl. *29*:197.

Miller, R.F., and M.M. Slaughter (1985) Excitatory amino acid receptors in the vertebrate retina. In W.W. Morgan (ed): Retinal Transmitters and Modulators: Models for the Brain. Boca Raton, FL: CRC Press, Vol. 2, pp. 123–160.

Murakami, M., and Y. Shimoda (1977) Identification of amacrine and ganglion cells in the carp retina. J. Physiol. (London) *264*:801–818.

Naka, K.-I. (1977) Functional organization of catfish retina. J. Neurophysiol. *40*:26–43.

Nawi, S., and D.R. Copenhagen (1987) Multiple classes of glutamate receptor on depolarizing bipolar cells in retina. Nature *325*:56–58.

Negishi, K., S. Kato, T. Teranishi, and M. Laufer (1978) Dual actions of some amino acids on spike discharges in the carp retina. Brain Res. *148*:67–84.

Nelson, R., E.V. Famiglietti Jr., and H. Kolb (1978) Intracellular staining reveals different levels of stratification for on- and off-center ganglion cells in the cat retina. J. Neurophysiol. *41*:472–483.

Rayborn, M.E., P.V. Sarthy, D.M.K. Lam, and J.G. Hollyfield (1981) The emergence, localization and maturation of neurotransmitter systems during development of the retina in *Xenopus laevis:* II. Glycine. J. Comp. Neurol. *195*:585–593.

Redburn, D.A., S.C. Massey, and P. Madtes (1983) The GABA uptake system in rabbit retina. In L. Hertz, E. Kvamme, E.G. McGeer, A. Schousboe (eds): Glutamine, Glutamate, and GABA in the Central Nervous System. New York: Alan R. Liss, Inc., pp. 273–286.

Saito, T., T. Kujiraoka, and J.-I. Toyoda (1984) Electrical and morphological properties of off-center bipolar cells in the carp retina. J. Comp. Neurol. *222*:200–208.

Saito, T., T. Kujiraoka, and T. Yanaha (1983) Connections between photoreceptors and horseradish peroxidase-injected bipolar cells in the carp retina. Vision Res. *23*:353–362.

Saito, T., T. Kujiraoka, T. Yanaha, and Y. Chino (1985) Reexamination of photoreceptor-bipolar connectivity patterns in carp retina: HRP-EM and golgi-EM studies. J. Comp. Neurol. *236*:141–160.

Sakai, H.M., K.-I. Naka, and J.E. Dowling (1986) Ganglion cell dendrites are presynaptic in catfish retina. Nature *319*:495–497.

Salpeter, M.M., F.A. McHenry, and E.E. Salpeter (1978) Resolution in electron microscope autoradiography IV. Application to analysis of autoradiographs. J. Cell Biol. *76*:127–145.

Slaughter, M.M., and R.F. Miller (1981) 2-Amino-4-phosphonobutyric acid: A new pharmacological tool for retina research. Science *211*:182–184.

Slaughter, M.M., and R.F. Miller (1983) An excitatory amino acid antagonist blocks cone input to sign-conserving second-order retinal neurons. Science *219*:1230–1232.

Studholme, K.M., and S. Yazulla (1987) Localization of endogenous GABA and glycine in goldfish retina by postembed EM immunocytochemistry. Invest. Ophthalmol. Vis. Sci. Suppl. *28*:349.

Studholme, K.M., and S. Yazulla (1988) Localization of glycine immunoreactivity in the goldfish retina. Invest. Ophthalmol. Vis. Sci. Suppl. *29*:273.

Tachibana, M., and Kaneko (1984) γ-Aminobutyric acid acts at axon terminals of turtle photoreceptors: Difference in sensitivity among cell types. Proc. Nat. Acad. Sci. USA *81*:7961–7964.

Teranishi, T., K. Negishi, and S. Kato (1984) Dye coupling between amacrine cells in the carp retina. Neurosci. Lett. *51*:73–78.

Teranishi, T., K. Negishi, and S. Kato (1985) Correlations between photoresponse and morphology of amacrine cells in the carp retina. Neurosci. Res. *52*:5211–5226.

Teranishi, T., K. Negishi, and S. Kato (1987) Functional and morphological correlates of amacrine cells in the carp retina. Neuroscience *20*:935–950.

Toyoda, J.-I., and M. Fujimoto (1984) Application of transretinal current stimulation for the study of bipolar-amacrine transmission. J. Gen. Physiol. *84*:915–925.

Toyoda, J.-I., and H. Hashimoto, and K. Ohtsu (1973) Application of transretinal current stimulation for the study of bipolar-amacrine transmission. Vision Res. *13*:295–307.

Vaughn, J.E., E.V. Famiglietti Jr., R.P. Barber, K. Saito, E. Roberts, and C.E. Ribak (1981) GABAergic amacrine cells in rat retina: Immunocytochemical identification of synaptic connectivity. J. Comp. Neurol. *197*:113–127.

Wong-Reilly, M., and G. Kageyama (1985) Cytochrome oxidase cytochemistry: Electron microscope analysis of serial post-fixation variables. Anat. Rec. *211*:217A.

Yazulla, S. (1981) GABAergic synapses in the goldfish retina: An autoradiographic study of ^{3}H-muscimol and ^{3}H-GABA binding. J. Comp. Neurol. *200*:83–93.

Yazulla, S. (1986) GABAergic mechanisms in the retina. In N. Osborne (ed): Progress in Retinal Research, Vol. 5. Oxford: Pergamon, pp. 1–52.

Yazulla, S., J. Mosinger, and C. Zucker (1984) Two types of pyriform Ab amacrine cells in the goldfish retina: An EM analysis of ^{3}H-GABA uptake and somatostatin-like immunoreactivity. Brain Res. *32*:352–356.

Yazulla, S., K. Studholme, and J.-Y. Wu (1986) Comparative distribution of ^{3}H-GABA uptake and GAD immunoreactivity in goldfish retinal amacrine cells: A double label analysis. J. Comp. Neurol. *244*:149–162.

Yazulla, S., K. Studholme, and J.-Y. Wu (1987) GABAergic input to the synaptic terminals of mb1 bipolar cells in the goldfish retina. Brain Res. *411*:400–405.